



1 **Modelling mussel (*Mytilus spp.*) microplastic accumulation.**

2

3 **Natalia Stamataki^{1,2,3}, Yannis Hatzonikolakis^{2,4}, Kostas Tsiaras², Catherine Tsangaris²,**
4 **George Petihakis³, Sarantis Sofianos¹, George Triantafyllou^{2,*}**

5

6 ¹Department of Environmental Physics, University of Athens, 15784 Athens, Greece

7 ²Hellenic Centre for Marine Research (HCMR), Athens-Sounio Avenue, MavroLithari, 19013 Anavyssos, Greece

8 ³Hellenic Centre for Marine Research (HCMR), 71003 Heraklion, Greece

9 ⁴Department of Biology, University of Athens, 15784, Greece

10

11 *Corresponding author: gt@hcmr.gr

12

13 **Abstract:** Microplastics (MPs) are a contaminant of growing concern due to their widespread
14 distribution and interactions with marine species, such as filter feeders. To investigate the MPs
15 accumulation by wild and cultured mussels, a Dynamic Energy Budget (DEB) model was
16 developed and validated with the available field data of *Mytilus edulis* (wild) from the North Sea
17 and *Mytilus galloprovincialis* (cultured) from the Northern Ionian Sea. Towards a generic DEB
18 model, the site-specific model parameter, half saturation coefficient (X_k) was applied as a power
19 function of food density for the cultured mussel, while for the wild it was calibrated to a constant
20 value. The DEB-accumulation model simulated the uptake and excretion rate of MPs, taking into
21 account environmental characteristics (temperature and chlorophyll-a). An accumulation of MPs
22 equal to 0.64 particles individual⁻¹ (fresh tissue mass 1.9 g) and 0.91 particles individual⁻¹ (fresh
23 tissue mass 3.4 g) was found for the wild and cultured mussel respectively, in agreement with the
24 field data. The inverse experiments investigating the depuration time of the wild and cultured
25 mussel in a clean from MPs environment showed a 90% removal of MPs load after 3 and 14 days,
26 respectively. Furthermore, sensitivity tests on model parameters and forcing functions highlighted
27 that besides MPs concentration, the accumulation is highly depended on temperature and
28 chlorophyll-a of the surrounding environment. For this reason, an empirical equation was found
29 relating directly the concentration of MPs in seawater, with MPs accumulation in mussel's soft
30 tissue, temperature and chlorophyll-a.

31



32 1. Introduction

33

34 Microplastic particles (MPs) are synthetic organic polymers with size below 5 mm (Arthur et
35 al., 2009) that originate from a variety of sources including mainly: those that are manufactured for
36 particular household or industrial activities, such as facial scrubs, toothpastes and resin pellets used
37 in the plastic industry (primary MPs), and those formed from the fragmentation of larger plastic
38 items (secondary MPs) (GESAMP, 2015). Eriksen et al. (2014) estimated that more than 5 trillion
39 microplastic particles, weighing over 250,000 tons, float in the oceans. Due to their composition,
40 density and shape, MPs are highly persistent in the environment and are, therefore, accumulating in
41 different marine compartments at increasing rates: surface and deeper layers in the water column, as
42 well as at the seafloor and within the sediments (Moore et al., 2001, Lattin et al., 2004, Thompson,
43 2004, Lusher, 2015). Since the majority of MPs entering the marine environment, originate from the
44 land (i.e. land-fills, littering of beaches and coastal areas, rivers, floodwaters, untreated municipal
45 sewerage, industrial emissions), the threat of MPs pollution in the coastal zone puts considerable
46 pressure on the coastal ecosystems (Cole et al., 2011, Andrady, 2011). In recent years, initiatives
47 under various projects (i.e. CLAIM, DeFishGear) target at evaluating the threat and impact of
48 marine litter pollution; the European framework of JERICO-RI focuses on a sustainable research
49 infrastructure in the coastal area to support the monitoring, science and management of coastal
50 marine areas (<http://www.jerico-ri.eu>). In the framework of JERICO-NEXT, a recent study
51 addressed the environmental threats and gaps in monitoring programmes in European coastal
52 waters, including the marine litter (i.e. MPs) as one of the most commonly identified threat to the
53 marine environment and highlighted the need for improved monitoring of the MPs distribution and
54 their impacts in European coastal environments (Painting et al., 2019).

55 Numerous studies have revealed that MPs are ingested either directly or through lower trophic
56 prey by animals from all levels of the food web; from zooplankton (Cole et al., 2013), small pelagic
57 fishes and mussels (Digka et al., 2018a) to mesopelagic fishes (Wieczorek et al., 2018) and large
58 predators like tuna and swordfish (Romeo et al., 2015). Microplastic ingestion by marine animals
59 can potentially affect animal health and raises toxicity concerns, since plastics can facilitate the
60 transfer of chemical additives and/or hydrophobic organic contaminants to biota (Mato et al., 2001,
61 Rios et al., 2007, Teuten et al., 2007, 2009, Hirai et al., 2011). Human, as a top predator, is also
62 contaminated by MPs (Schwabl et al., 2019). Mussel and small fishes that are commonly consumed
63 whole, without removing digestive tracts, where MPs are concentrated, are among the most likely
64 pathways for MPs to embed in the human diet (Smith et al., 2018). Especially regarding marine
65 organisms (i.e. mussels), it is notable that the levels of their contamination has been added to the



66 European database (www.ecsafeseafooddbase.eu) as an environmental variable of growing concern,
67 reflecting the health status (Marine Strategy Framework Directive (MSFD) Descriptor 10 – Marine
68 Litter (Decision 2017/848/EU)) (De Witte et al., 2014, Vandermeersch et al., 2015, Digka et al.,
69 2018a). Today, a series of studies have denoted the presence of MPs in mussels' tissue intended for
70 human consumption (Van Cauwenberghe and Janssen, 2014, Mathalon and Hill, 2014, Li et al.,
71 2016, 2018, Hantoro et al., 2019). For instance, in a recent study, Li et al. (2018) sampled mussels
72 from coastal waters and supermarkets in the U.K and estimated that a plate of 100g mussels
73 contains 70 MPs that will be ingested by the consumer. The presence of MPs in mussels has been
74 also demonstrated during laboratory trials in their faeces, intestinal tract (Von Moos et al., 2012,
75 Van Cauwenberghe et al., 2015, Wegner et al., 2012, Khan and Prezant, 2018), as well as in their
76 circulatory system (Browne et al., 2008). Other laboratory studies showed several effects of
77 microplastic ingestion in laboratory exposed mussels, including histological changes, inflammatory
78 responses, immunological alterations, lysosomal membrane destabilization, reduced filtering
79 activity, neurotoxic effects, oxidative stress effects, increase in hemocyte mortality, dysplasia,
80 genotoxicity and transcriptional responses (reviewed by Li et al., 2019). However, the tested
81 concentrations of MPs in laboratory experiments are frequently unrealistic, being several orders of
82 magnitude higher (2 to 7 orders of magnitude) than the observed seawater concentrations (Van
83 Cauwenberge et al., 2015, Lenz et al. 2016).

84 Mussels, through their extensive filtering activity, feed on planktonic organisms that have
85 similar size with MPs (Browne et al., 2007) and considering also their inability to select particles
86 with high energy value (i.e. phytoplankton) during filtration (Vahl, 1972, Saraiva et al., 2011a),
87 they are directly exposed to MPs' contamination. Recent studies suggest a positive linear
88 correlation between MPs concentration in mussels and surrounding waters (Capolupo et al., 2018,
89 Qu et al. 2018, Li et al. 2019). The filtering activity of mussels, which directly affects the resulting
90 MPs accumulation, is a complicated process that is controlled by other factors (food availability,
91 temperature, tides etc.).

92 The purpose of the present work is to study the accumulation of MPs by the mussel and reveal
93 relations between accumulated concentrations in mussels' soft parts and environmental features. In
94 this context, an accumulation model was developed based on Dynamic Energy Budget theory
95 (DEB, Kooijman, 2000) and applied in two different regions, in two different modes of life (wild
96 and cultivated): in the North Sea (*M. edulis*, wild) and in the Northern Ionian Sea (*M.*
97 *galloprovincialis*, cultivated). DEB theory provides all the necessary detail to model the feeding
98 processes and aspects of the mussel metabolism, taking into account the impact of the
99 environmental variability on the simulated individual. Apart from modeling the growth of bivalves
100 (Rosland et al., 2009, Sara et al., 2012, Thomas et al., 2011, Saraiva et al., 2012, Hatzonikolakis et



101 al., 2017, Monaco & McQuaid, 2018), DEB models have been used to study other processes as
102 well, such as bioaccumulation of PCBs (Polychlorinated Biphenyls) and POPs (Persistent Organic
103 Compounds) (Zaldivar, 2008), trace metals (Casas and Bacher, 2006) and the impact of climate
104 change on individual's physiology (Sara et al., 2014). However, to our knowledge this is the first
105 time that a DEB-based model is used to assess the uptake and excretion rates of MPs in mussels.

106
107

108 **2. Materials and Methods**

109

110 **2.1 Study areas and field data**

111

112 The North Sea is a large semi-enclosed sea on the continental shelf of north-west Europe with
113 a total surface area of 850,000 km² and is bounded by the coastlines of 9 countries. The sea is
114 shallow (mean depth 90 m), getting deeper towards the north (up to 725 meters) and the semi-
115 diurnal tide (tidal range 0-5 m) is the dominant feature of the region (Otto et al., 1990). Major
116 rivers, such as Rhine, Elbe, Weser, Ems and Thames discharge into the southern part of the sea
117 (Lacroix et al., 2004), making this area a productive ecosystem. In this study, the area is limited
118 along the French, Belgian and Dutch North Sea coast (N 50.98°-51.46°, W 1.75°-3.54°). This is
119 located close to harbors, where shipping, industrial and agricultural activity is high, putting
120 considerable pressure on the ecological systems of the region (Van Cauwenberghe et al., 2015).

121 The MPs concentration in mussels' tissue and seawater that were used to validate and force
122 the model respectively at its North Sea implementation were derived from Van Cauwenberghe et al.
123 (2015). Van Cauwenberghe et al. (2015) examined the presence of MPs in wild mussels (*M. edulis*),
124 and thus collected both biota and water at 6 sampling stations along the French, Belgian and Dutch
125 North Sea coast in late summer of 2011. *M. edulis* (mean shell length: 4 ± 0.5 cm and wet weight
126 (w.w.): 2 ± 0.7 g) and water samples were randomly collected on the local breakwaters, in order to
127 assess the MPs concentration in the organisms and their habitat. MPs were present in all analyzed
128 samples, both organisms and water. Seawater samples (N=12) had MPs (<1mm) on average 0.4 ±
129 0.3 particles L⁻¹ (range: 0.0 – 0.8 particles L⁻¹) and *M. edulis* contained on average 0.2 ± 0.3
130 particles g⁻¹w.w. (or 0.4 ± 0.3 particles individual⁻¹) (Van Cauwenberghe et al., 2015). The size
131 range of MPs found within the mussels was 20-90 µm (size <1 mm).

132 The Northern Ionian Sea is located in the transition zone between the Adriatic and Ionian Sea.
133 The long and complex coastline, presents a high diversity of hydrodynamic and sedimentary



134 features. Rivers discharging into the Northern Ionian Sea include Kalamas/Thyamis (Greece) and
135 Butrinto (Albania) (Skoulikidis et al., 2009), making the area suitable for aquaculture. Small
136 farming sites and shellfish grounds are operating in Thesprotia (northwestern Ionian Sea)
137 (Theodorou et al., 2011). The main source of marine litter inputs in the area originates from
138 anthropogenic activities that mainly include shoreline tourism and recreational activities, poor
139 wastewater management, agricultural practices, fisheries, aquacultures and shipping (Vlachogianni
140 et al., 2017; Digka et al., 2018a). According to Politikos et al. (2020), the area around the Corfu
141 island (Northern Ionian Sea) is characterized as a retention area of litter particles probably due to
142 the prevailing weak coastal circulation. Furthermore, a northward current on the east Ionian Sea
143 facilitates the transfer of litter particles towards the Adriatic Sea, which has been characterized as a
144 hotspot of marine litter and one of the most affected areas in the Mediterranean Sea (Pasquini et al.,
145 2016, Vlachogianni et al., 2017, Liubartseva et al., 2018, Politikos et al., 2020).

146 The field data used to validate the model output in the N. Ionian Sea were obtained from
147 Digka et al. (2018b, 2018a). In the framework of the “DeFishGear” project, mussels (*M.*
148 *galloprovincialis*) were collected by hand from a long line type mussel culture farm in Thesprotia
149 (N 39.606567° E 20.149421°), in summer 2015 (July) at a sampling depth up to 3 m (Digka et al.,
150 2018a). The average MPs accumulation was calculated from a total population of 40 mussels
151 originated from the farm, with 18 of them found contaminated with MPs (46.25%). The average
152 load of MPs (size <1 mm) per mussel (mean shell length 5.0 ± 0.3 cm) was 0.9 ± 0.2 particles
153 individual⁻¹ and the size of MPs found in the mussel’s tissue ranged from 55 to 620 μm . Both clean
154 and contaminated mussels were included in the calculated mean value in order to represent the
155 mean state of the contamination level for the individual inhabiting the study area.

156 The seawater concentration of MPs for the N. Ionian Sea implementation was obtained from
157 Digka et al. (2018b) and the DeFishGear project results ([http://www.defishgear.net/project/main-](http://www.defishgear.net/project/main-lines-of-activities)
158 [lines-of-activities](http://www.defishgear.net/project/main-lines-of-activities)). In total, 12 manta net tows were conducted in the region, collecting a total
159 number of $n_1=2,027$ particles on October 2014 and $n_2=1,332$ on April 2015, leading to an average
160 of 280 particles per tow with size <1 mm and >330 μm (Digka et al., 2018b). In order to estimate
161 the mean MPs concentration in the region, expressed as particles per volume, the dimensions of the
162 manta net (W 60 cm H 24 cm, rectangular frame opening, mesh size 330 μm) and the sampling
163 distance of each tow (~2 km) were used by multiplying the sample surface of the net by the trawled
164 distance in meters (Maes et al., 2017), which resulted in a mean MPs concentration of 1.17 particles
165 m^{-3} (233,333 particles km^{-2}). Moreover, in the wider region of the Adriatic Sea, Zeri et al. (2018)
166 found a mean density of $315,009 \pm 568,578$ particles km^{-2} (1.58 ± 2.84 particles m^{-3}), out of which
167 34% sized <1 mm. A relatively high value of standard deviation (one order of magnitude higher
168 than the mean value) is adopted (0.0012 ± 0.024 particles L^{-1}), considering that the mussel farm is



169 established in an enclosed gulf and close to the coast, since, according to Zeri et al. (2018), the
170 abundance of MPs is one order of magnitude higher in inshore (<4 km) compared to offshore
171 waters (>4 km). Furthermore, it may be assumed that the adopted range (standard deviation is also
172 multiplied by a factor of 2) includes also the smaller particles sized between 50 μm and < 330 μm ,
173 which have been found in mussel's tissue (Digka et al., 2018a), but were overlooked during the
174 seawater sampling due to the manta net's mesh size (> 330 μm). According to Enders et al. (2015)
175 the relative abundance of small particles (50- 300 μm) compared to particles larger than 300 μm is
176 approximately 50%.

177

178 2.2 DEB model description

179

180 In the present study, a Dynamic Energy Budget (DEB, Kooijman, 2000, 2010) model is used
181 as basis to simulate the accumulation of MPs by mussels. In DEB theory (Kooijman, 2000), the
182 energy assimilated through food by the simulated individual is stored in a reserve compartment
183 from where a fixed energy fraction κ is allocated for growth and somatic maintenance, with a
184 priority for maintenance. The remaining energy ($1 - \kappa$) is spent on maturity maintenance and
185 reproduction. The individual's condition is defined by the dynamics of three state variables: energy
186 reserves E (joules), structural volume V (cm^3) and energy allocated to reproduction R (joules). The
187 energy flow through the organism is controlled by the fluctuations of the available food density and
188 temperature characterizing the surrounding environment.

189 The DEB model implemented here is an extended version of the model described in
190 Hatzonikolakis et al. (2017), where the growth of the Mediterranean mussel is simulated by taking
191 into account only the assimilation rate of the individual. Since the present study focuses on
192 simulating the MPs accumulation, it is crucial to include a detailed representation of the mussel's
193 feeding mechanism. In this context, the DEB model was extended by including the clearance (C_r),
194 filtration (\dot{p}_{XIF}) and ingestion (\dot{p}_{XII}) rates of the mussel, following Saraiva et al. (2011a), with MPs
195 represented by the silt variable. In this approach, a pre-ingestive selection occurs between filtration
196 and ingestion, returning the rejected material in the water through pseudofaeces (J_{pfi}).
197 Consequently, energy is assimilated through food while the non-assimilated particles are excreted
198 through the faeces production (J_f). The model's equations, variables and parameters are shown in
199 Table 1, 2 and 3 respectively. The scaled functional response f (Eq. 5, Table 1), which regulates the
200 assimilation rate, is modified following Kooijman (2006) to include an inorganic term representing
201 the non-digestible matter i.e. microplastics: $f = X/(X + K_y)$ and $K_y = X_K \cdot (1 + Y/Y_K)$ where Y
202 and Y_k are the concentration of MPs, converted from particles L^{-1} to g m^{-3} (Everaert et al., 2018) and



203 the half saturation coefficient of inorganic particles here represented by MPs (g m^{-3}), respectively.
204 Thus, the assimilation rate that is regulated by f is decreasing when the concentration of MPs is
205 increased. The same approach is followed by other authors who considered inedible particles in the
206 mussel's diet (Ren, 2009, Troost et al., 2010). During the filtration process the same clearance rate
207 for all particles is used ($\{\dot{C}_R\}$), representing the same searching rate for food that depends on the
208 organism maximum capacity ($\{\dot{C}_{Rm}\}$) and environmental particle concentrations (Vahl, 1972,
209 Widdows et al., 1979, Cucci et al., 1989). During the ingestion process the mussel is able to
210 selectively ingest food particles and reject inedible material, in order to increase the organic content
211 of the ingested material ((Kjørboe & Møhlenberg, 1981, Jørgensen et al., 1990, Prins et al., 1991,
212 Maire et al., 2007, Ren, 2009, Saraiva et al., 2011a). This selection is reflected by the different
213 binding probabilities adopted for each type of particle (ρ_1 for algae particles and ρ_2 for inorganic
214 particles i.e. MPs, see Eq. 14 and table 3). The equations representing the feeding processes handle
215 each type of particle separately, while there is interference between the simultaneous handling of
216 different particle types (Eq. 12-14, Table 1) (Saraiva et al., 2011a). Finally, during the assimilation
217 process, suspended matter (i.e. MPs) that the mussel is not able to assimilate due to its different
218 chemical composition from the reserve compartment (Saraiva et al., 2011a) or incipient saturation
219 at high algal concentrations (Riisgard et al., 2011) results in the faeces production (Eq. 16, Table 1).
220

221 **2.3 Microplastics accumulation sub-model**

222

223 With the DEB model as a basis, a sub-model describing the microplastics (MPs) accumulation
224 by the mussel was developed, assuming that the presence of MPs in the ambient water does not
225 cause a significant adverse effect on the organisms' overall energy budget, in accordance with
226 laboratory experiments, conducted in mussel species (Van Cauwenberghe et al., 2015: *Mytilus*
227 *edulis*, Santana et al., 2018: mussel *Perna perna*). Additionally, it was assumed that the mussel
228 filtrates MPs present in the water, without the ability of selecting between the high energetic valued
229 particles and the MPs during the filtration process (Van Cauwenberghe et al., 2015, Von Moos et
230 al., 2012, Browne et al., 2008, Digka et al., 2018a among others). The uptake of MPs from the
231 environment is taken into account through the process of clearance/filtration rate, while the
232 excretion of the contaminant is derived from two processes: (i) pseudofaeces production and (ii)
233 faeces production. The resulting MPs accumulation is influenced by external environmental factors
234 (MPs concentration, food availability, temperature) and internal biological processes (clearance,
235 filtration, ingestion, growth). All these are described by the following differential equation:

236



$$237 \quad \frac{dC}{dt} = C_{env} \cdot \dot{C}_R - \int_{pf2} - \frac{J_f}{p_{X1I}} \cdot C \quad (\text{Eq. 18})$$

238 where \dot{C}_R is the clearance rate for water ($L h^{-1}$), containing a concentration of MPs C_{env} (particles L^{-1}). The terms of \int_{pf2} and $\frac{J_f}{p_{X1I}}$ represent the elimination rate of MPs through pseudofaeces and the
239 1). The terms of \int_{pf2} and $\frac{J_f}{p_{X1I}}$ represent the elimination rate of MPs through pseudofaeces and the
240 non-dimensional rate of faeces production with respect to the ingestion rate, respectively (see Table
241 1, Eq. 15-16). In this context, the pseudofaeces production incorporates the rejected MPs prior to
242 the ingestion, while the faeces production includes MPs that are rejected along with the food
243 particles that are not assimilated by the mussel.
244 The accumulation of MPs in the individual is represented by the state variable C (particles
245 individual $^{-1}$) which is computed at every model time step. This has been set to one hour, in order to
246 properly resolve the dynamics of the rapidly changing processes, such as feeding and excretion.

247 **2.4 Environmental drivers**

248

249 Besides MPs concentration in the seawater, the DEB model is forced by sea surface
250 temperature (SST) and food availability, defined as chlorophyll-a concentration (CHL-a).
251 Hatzonikolakis et al. (2017) have tested the performance of the model, considering also particulate
252 organic carbon (POC) in the mussel's diet, which, however, did not have an important impact on
253 the model's skill against field data. Thus, only CHL-a, is considered as the available food source.
254 For both study areas SST and CHL-a are derived from daily satellite data, a method also used by
255 other authors (i.e. Thomas et al., 2011, Monaco & McQuaid, 2018).

256 In the North Sea, SST data were obtained from daily satellite images provided by Copernicus
257 Marine Environmental Monitoring Service (CMEMS) at 0.04 degree spatial resolution and CHL-a
258 data from the daily multi-sensor product provided by CMEMS- Globcolour database at 1 km spatial
259 resolution (<http://marine.copernicus.eu/>, generated using CMEMS Products, production center
260 ACRI-ST). The environmental forcing data (SST, CHL-a) were averaged over the study area
261 (51.08° - 51.44° N, 2.19° - 3.45° E), covering the period 2007-2011 (5 years), in order to realistically
262 simulate the wild mussel's growth harvested at late summer 2011 (Van Cauwenberghe et al., 2015).

263 In the North Ionian Sea, daily satellite SST data were also obtained from the CMEMS
264 database for the Mediterranean Sea with 0.04 degree spatial resolution, while CHL-a data were
265 derived from the merged product of many satellites (i.e. SeaWiFs, Meris, Modis, Viirs and Olci-a)
266 provided by Globcolour web interface (<http://globcolour.info>) at a daily temporal resolution and 1
267 km spatial resolution. The forcing data were averaged over the study area ($N 39.49^{\circ}$ - 39.65° , E
268 20.09° - 20.23°) covering the period 2014-2015 (2 years), when the cultured mussel is ready for the
269 market. The satellite derived CHL-a data were estimated based on the OC5 algorithm of Gohin et



270 al. (2002) in both study areas, which is regarded as suitable for coastal waters. Satellite data have
271 facilitated large scale ecological studies by providing maps of phytoplankton functional types and
272 sea surface temperature (Raitsos et al., 2005, 2008, 2012, 2014, Palacz et al., 2013). The daily
273 environmental forcing data are shown in Fig. 1 and Fig. 2 for the North Sea and the N. Ionian Sea,
274 respectively. The two coastal environments present some important differences regarding both
275 CHL-a and SST. Specifically, in the N. Ionian Sea, CHL-a is relatively low (annual mean ~ 0.88 mg
276 chl-a m^{-3}) and peaks during winter (maximum ~ 2.64 mg chl-a m^{-3} at December 2014), while in the
277 North Sea CHL-a is about four times higher (annual mean 4.25 mg chl-a m^{-3}), peaking in April
278 every year (maximum range 29.44 - 33.38 mg chl-a m^{-3}), as soon as light availability reaches a
279 critical level (Van Beusekom et al., 2009). The higher productivity in the North Sea is related with
280 the nutrient inputs from the English Channel, the North Atlantic and particularly the river discharge
281 of nutrient-rich waters along the Belgian-French-Dutch coastline, that peaks during winter period
282 (Van Beusekom et al., 2009). The sea surface temperature peaks during August in both areas (Fig. 1
283 and Fig. 2), but is significantly higher in the N. Ionian Sea (maximum $28.8^{\circ}C$), as compared to the
284 North Sea (maximum 18 - $19.3^{\circ}C$).

285 The environmental concentration of MPs, C_{env} (particles L^{-1}) was obtained also at a daily time
286 step as randomly generated values of the Gaussian distribution that is determined by the mean value
287 and standard deviation of the observed field data (0.4 ± 0.3 particles L^{-1} , North Sea, Van
288 Cauwenberghe et al., 2015, 0.0012 ± 0.024 particles L^{-1} , N. Ionian Sea, Digka et al., 2018a).
289 Considering that these values originate from surface waters and that mussels live in the near surface
290 layer (0-5 m), C_{env} is estimated as a mean value of the upper layer with the methods described by
291 Kooi et al. (2016), who studied the vertical distribution of MPs, considering an exponential
292 decrease with depth. Specifically, in the N. Ionian Sea, mussels were collected from a depth up to 3
293 m (Digka et al., 2018a), while in the North Sea (Van Cauwenberghe et al., 2015), there is no
294 information and thus a maximum depth of 5 m is adopted.

295 In the North Sea simulation, the effect of tides is taken into account by considering that the
296 mussel originated from the intertidal zone, is submerged 12 hours during the day (Van
297 Cauwenberghe et al., 2015). In the N. Ionian Sea simulation, tides are not considered, given the
298 very small tide amplitude (few centimeters) in the Mediterranean (i.e. Sara et al., 2011;
299 Hatzonikolakis et al., 2017) and thus the cultured mussel is assumed permanently submerged. *In*
300 *situ* hourly tide data (2007-2011) from the coastal zone of the region (Dunkerque station N
301 51.04820° , E 2.36650°) obtained from Coriolis and Copernicus data provider
302 (<http://marine.copernicus.eu>, <http://www.coriolis.eu.org>), showed that mussels experience
303 alternating periods of aerial exposure and submergence at approximately every 6 hours (2 high and
304 2 low tides). During aerial exposure the model suspends the feeding processes (Sara et al., 2011)



305 and simulates metabolic depression (Monaco & McQuaid, 2018) where, the Arrhenius thermal
306 sensitivity equation (Eq. 9) is corrected by a metabolic depression constant ($M_d = 0.15$), a value
307 representative for *M. galloprovincialis* and here applied also for *M. edulis*. In the present study, the
308 mussel's body temperature change during low tide is ignored, inducing a model error. The mussel's
309 body temperature (i.e. surrounding water temperature for submerged mussels) during air exposure
310 depends on many factors, such as solar radiation, air's temperature, wind speed and wave height,
311 according to studies investigating the temperature effect on intertidal mussels (Kearney et al., 2010,
312 Sara et al., 2011). However, the present study aims to primarily examine the MPs accumulation and
313 thus the intertidal mussel's body temperature was not thoroughly examined. Nonetheless, the time
314 that the mussel is able to filter, ingest and excrete the suspended matter (i.e. food and MPs particles)
315 and the effect on the mussel's growth through the modified relation of $k(T)$ are included, since the
316 assimilation process occurs whether the mussel is submerged or not (Kearney et al., 2010).

317 2.5 Parameter values

318

319 Most of the DEB model parameters were obtained from Van der Veer et al. (2006) and are
320 referred to the blue mussel *Mytilus edulis* in the northeast Atlantic (see Table 3 for the exceptions).
321 This assumption has also been adopted in previous studies which showed that this parameter set for
322 *M. edulis* applies also for *M. galloprovincialis* (i.e. Casas and Bacher, 2006, Hatzonikolakis et al.,
323 2017). The half saturation coefficient X_k represents the density of food at which the food uptake rate
324 reaches half of its maximum value and should be treated as a site – specific parameter (Troost et al.,
325 2010, Pouvreau et al., 2006). In order to estimate the value of X_k , a different approach was followed
326 for each study area.

327 For the North Sea simulation, X_k was tuned so that the simulated individual has the recorded
328 size at the corresponding estimated age (Van Cauwenberghe et al., 2015) growing with the
329 representative growth rates of wild *M. edulis* at the region (Saraiva et al., 2012, Sukhotin et al.,
330 2007). For the N. Ionian Sea simulation, an alternative method was adopted, aiming to generalize
331 the DEB model to overcome the problem of site-specific parameterization. The DEB model was
332 tuned against literature field data for cultured mussels originated from different areas in the
333 Mediterranean and Black Seas, where the average CHL-a concentration ranged between 1.0 and 5.0
334 mg chl-a m^{-3} , and one X_k value was found for each area. The four areas used, their characteristics
335 and the corresponding value of X_k adopted, are shown in Table 4. These values of X_k are related to
336 the prevailing CHL-a concentration of each area ([CHL-a]) through three different functions:
337 linear: $f(x) = a * [CHL - a] + b$ exponential: $f(x) = a * \exp(b * [CHL - a])$ and power: $f(x) =$
338 $a * [CHL - a]^b + c$. The curve fitting app of Matlab (Matlab R2015a) was used for the



339 determination of a, b and c of each function taking into account the 95% confidence level. The
340 score of each function regarding the somatic/mussel growth simulation in all four regions is tested
341 through target diagrams (Jolliff et al., 2009) by computing the bias and unbiased root-mean-square-
342 deviation (RMSD) between field and simulated data of all 4 regions and the function with the best
343 score is adopted. A similar approach was followed by Alunno-Bruscia et al. (2011) for the oyster
344 *Crassostrea gigas* in six Atlantic ecosystems who expressed the X_k as a linear function of food
345 density (e.g. phytoplankton). Unfortunately, the approach described for the N. Ionian Sea
346 simulation could not be applied in the North Sea, as the limited amount of growth data from the
347 literature for wild *M. edulis* in similar environments did not permit a statistically significant fit of a
348 similar function ($X_k = f(chl - a)$).

349

350 **2.6 Simulation of reproduction-Initialization of the model**

351

352 The reproductive buffer (R) is assumed to be completely emptied at spawning ($R = 0$)
353 (Sprung, 1983, Van Haren et al., 1994). In order to simulate mussel's spawning, the gonado-somatic
354 index (GSI) defined as gonad dry mass over total dry flesh mass was computed at every model's
355 time step (Eq. 17 Table 1; the water content of the fresh tissue mass was assumed 80% according to
356 Thomas et al. (2011)). Spawning was induced by a critical value of GSI (GSI_{th} , Table 3) and a
357 minimum temperature threshold (T_{th}) at each study area, obtained from the literature. In the North
358 Sea implementation, T_{th} was set at 9.6 °C (Saraiva et al., 2012), while in the N. Ionian Sea, at 15 °C
359 (Honkoop and Van der Meer, 1998). This kind of formulation for the spawning event in bivalves
360 has been used in previous studies (i.e. Pouvreau et al., 2006, Troost et al., 2010, Thomas et al.,
361 2011, Monaco & McQuaid, 2018). The simulated abrupt losses of the mussel's tissue mass
362 correspond to spawning events and the model's prediction was compared with the available
363 literature data regarding the spawning period in each study area. Theodorou et al. (2011)
364 demonstrated that the spawning events occur during winter for *M. galloprovincialis* in the mussel
365 farms of Greece, while in the North Sea the spawning period for *M. edulis* is extended from the end
366 of April until the end of June (Sprung, 1983, Cardoso et al., 2007).

367 In both areas, the model was initialized so that the simulated individual is in the juvenile phase
368 ($V < V_p$; Table 3) and the reproductive buffer can be considered to be empty ($R = 0$) (Thomas et al.,
369 2011). As stated by Jacobs et al. (2015) amongst others, juvenile mussels (*M. edulis*) range between
370 1.5-25 mm in size. Specifically, in the North Sea the settlement of mussel larvae (*M. edulis*) takes
371 place in June and the juveniles grow to a maximum size of 25 mm within 4 months (Jacobs et al.,
372 2014). In the N. Ionian Sea, the operating mussel farms follow the life cycle of *M.*



373 *galloprovincialis*, starting the operational cycle each year by dropping seed collectors from late
374 November until March and the juvenile mussels grow up to 6-6.5cm after approximately one year
375 according to the information obtained from the local farms in the region and Theodorou et al.
376 (2011). The initial fresh tissue mass was distributed between the structural volume (V) and reserves
377 energy (E). Energy allocated to those two compartments was firstly constrained by the initial length
378 (L) and then energy allocated to V was in Eq.10 (Table 1). The initial value of E was set so that the
379 simulated individual has an initial weight that corresponds to the juvenile phase ($V < V_p$) (Table 5).
380 Finally, for both model implementations, the initial accumulation of MPs in the mussel's tissue (C)
381 was set to zero.

382

383 2.7 Simulation Runs

384 The DEB-accumulation model simulates at an hourly basis the growth and MPs accumulation
385 of the wild mussel from the North Sea and the cultured mussel from the N. Ionian Sea. Initially, a
386 model run is performed at each study area during the periods July 2007 to August 2011 (4 years) for
387 the North Sea simulation and late November 2014 to January 2016 (~ 1 year) for the N. Ionian Sea
388 simulation. Additionally, the inverse simulations were performed in order to evaluate the depuration
389 phase of both cultured and wild mussel, by setting the environmental MPs concentration equal to
390 zero ($C_{env}=0$), after a period of 1 year simulation at the N. Ionian Sea, when the cultured mussel has
391 the appropriate size for market, and after 4 years at the North Sea, when literature field data are
392 available (Van Cauwenberghe et al., 2015). In this simulation, the mussel's gut clearance is
393 achieved by the excretion of MPs through faeces (3rd term of Eq. 18), and thus it is necessary to
394 maintain the existence of food in the mussel's environment in order to ensure that the feeding-
395 excretion processes will occur.

396 Furthermore, to examine the model's uncertainty related to the environmental MPs
397 concentration, a series of 15 and 13 simulations were performed in the North Sea and N. Ionian Sea
398 respectively, adopting different constant values of C_{env} within the observed range of each area.
399 Finally, the effect of the environmental forcing data and some model's parameters on the resulting
400 MPs accumulation by both mussels is explored through sensitivity experiments. These were used to
401 derive a new function that predicts the level of MPs pollution in the environment.

402

403 2.8 Sensitivity tests and Regression analysis



404 The effect of the environmental data (CHL-a, temperature, C_{env}) and two parameters
405 representative of mussel's growth (X_k , Y_k) on the MPs accumulation by the mussel for each study
406 area was examined through sensitivity experiments with the DEB-accumulation model. Each
407 variable (CHL-a, T, C_{env}) and parameter (X_k , Y_k) was perturbed by $\pm 10\%$ and the results of each run
408 were analyzed using the sensitivity index (SI), which calculates the percentage change of the
409 mussel's MPs accumulation $SI = \frac{1}{n} \sum_{t=1}^n \frac{|C_t^1 - C_t^0|}{C_t^0} \cdot 100$ (%), where n is the simulated time steps, C_t^0
410 is the MPs accumulation predicted with the standard simulation at time t and C_t^1 is the MPs
411 accumulation with a perturbed variable/parameter at time t ; for details see Bacher and Gangnery,
412 (2006). In order to also examine the effect of tides, in the North Sea implementation, the sensitivity
413 experiments were conducted twice: the first time assuming that the mussel is permanently
414 submerged and the second time assuming that the mussel is periodically exposed to the air.

415 Preliminary sensitivity experiments showed that the MPs accumulation is highly depended on
416 the prevailing conditions regarding the CHL-a, temperature and C_{env} and the mussel's growth that is
417 regulated by the half saturation coefficient (X_k). Therefore an attempt was made using the model's
418 output to describe the MPs accumulation as a function of these variables through a custom
419 regression model:

$$420 \quad y = b_1 * W + b_2 * \exp\left(\frac{1}{T}\right) + b_3 * \frac{1}{[CHL-a]} + b_4 * C_{env} \quad (\text{Eq. 19})$$

421 where y (particles/individual) is the response variable and represent the predicted MPs
422 accumulation by the mussel; W (g) the mussel's fresh tissue mass, T (K) the sea surface
423 temperature, CHL-a and C_{env} are the concentrations of chlorophyll-a and MPs in the water
424 respectively, which are the predictor variables. The values of coefficients b_1 , b_2 , b_3 , and b_4 are
425 calculated using the nonlinear regression function (nlinfit, Matlab R2015a) which attempts to find
426 values of the parameters b that minimize the least squared differences between the model's MPs
427 accumulation output C and the predictions of the regression model $y = f(W, T, [chl\ a], C_{env}, b)$.

428 The ultimate aim of this analysis, once coefficients are determined, is to use equation 19 to
429 obtain the environmental MPs concentration:

$$430 \quad C_{env} = \frac{1}{b_4} * \left(C - b_1 * W - b_2 * \exp\left(\frac{1}{T}\right) - b_3 * \frac{1}{[CHL-a]} \right) \quad (\text{Eq. 20})$$

431

432 which could be a very useful tool to predict the MPs concentration in the environment, when all
433 involved variables are known (mussel size, accumulated MPs, temperature and CHL-a), using the



434 mussel as a potential bioindicator (Li et al., 2016, Li et al., 2019). The score of this custom model
435 was tested by applying Eq. 20 in our study areas and 6 more areas around the U.K., where
436 information of mussel's wet weight and both mussels' and environment's MPs load is available (Li
437 et al., 2018). CHL-a and temperature, which were not included in Li et al. (2018), were obtained
438 from daily satellite images (same source as in the North Sea, see 2.4 section), covering the period
439 that the mussels were harvested (Li et al., 2018).

440

441 **3. Results**

442

443 **3.1 Growth simulations**

444

445 The growth simulations of *M. edulis* and *M. galloprovincialis* for the North Sea and the N.
446 Ionian Sea are shown in Fig. 4 and Fig. 5 respectively. In the North Sea implementation, X_k was
447 tuned to a constant value: $X_k=8$ mg chl-a m^{-3} . The fitted value was slightly higher, as compared to
448 the one ($X_k=3.88$ μg chl-a l^{-1}) used by Casas and Bacher (2006) in productive areas of the French
449 Mediterranean shoreline (average CHL-a concentration 1.45 μg chl-a l^{-1} maximum peak at 20 μg
450 chl-a l^{-1}), given the even higher productivity in the North Sea (average CHL-a concentration 4.25
451 μg chl-a l^{-1} ; maximum peak at ~ 33.40 μg chl-a l^{-1}). The high value of X_k could also be explained by
452 the presence of silt and other inedible particles (i.e. MPs) which result to lower quality food in the
453 mussel's diet compared with a "clean" site (Kooijman, 2006, Ren, 2009). Furthermore, it has been
454 reported that wild mussels grow considerably slower than farmed mussels (~ 1.7 times) (Sukhotin
455 and Kulakowski, 1992) and thus, a higher value of X_k promotes a lower mussel growth, which is the
456 case of the North Sea mussel. The simulated mussel shell length after 4 years, in August, is 4.35 cm
457 and the fresh tissue mass is 1.87 gr, in agreement with Van Cauwenberghe et al. (2015) and other
458 studies conducted on wild mussels (Sukhotin et al., 2007, Saraiva et al., 2012, MarLIN, 2016). In
459 particular, Saraiva et al. (2012) found that after 16 years of simulation, the wild mussel of the
460 Wadden Sea (North Sea) is 7 cm long, while according to Bayne and Worrall (1980) a mussel with
461 shell length 4 cm corresponds to the age of 4 years, in agreement with the current study. The
462 simulated growth presents a strong seasonal pattern, being higher during spring and summer season,
463 as compared to autumn and winter, which is consistent with the seasonal cycle of temperature and
464 CHL-a concentration, for a typical year in the region (Fig. 1). The increase of food availability and
465 temperature during spring (April) results in high mussel growth for a 4-month period, while the
466 decrease of CHL-a from summer until the end of the year, in conjunction with the temperature



467 decrease in autumn, result in a lower mussel growth. Spawning events occurred between the end of
468 April and beginning of May (30 April-2 May) each year, are responsible for the sharp decline in
469 mussel's fresh tissue mass, shown in Fig. 4 (Handa et al., 2011; Zaldivar, 2008) and in agreement
470 with the literature (Sprung, 1983, Cardoso et al., 2007, Saraiva et al., 2012). The predicted weight
471 loss due to spawning was around 7% at the first year of simulation, while the second, third and
472 fourth year the percentage of weight loss increased gradually to 8.3%, 12.6% and 14.4%
473 respectively. Bayne and Worrall (1980) demonstrated that the weight losses on spawning for
474 individuals of 1 g weight vary between 2.1% and 39.8%, presenting a weight-specific increase with
475 size.

476 In the N. Ionian Sea implementation, X_k is applied as a function of CHL-a concentration
477 through the method described in section 2.5. The target diagram showing the performance of each
478 tested function (linear: $f(x) = a * [CHL - a] + b$, where $a = 0.959$ and $b = -1.420$; exponential:
479 $f(x) = a * \exp(b * [CHL - a])$ where $a = 0.2$ and $b = 0.567$; power: $f(x) = a * [CHL - a]^b +$
480 c where $a = 0.01$, $b = 3.529$ and $c = 0.480$) is shown in figure 3. The linear and power function
481 of X_k present a good skill, with the power function leading to the most successful simulation of the
482 cultured mussel's growth in all four areas (diagram marks for mussel length and fresh tissue mass
483 are closer to the target's center). The power function applied in the N. Ionian Sea, resulted in
484 mussel's shell length 5.8 cm and fresh tissue mass 5.92 gr after one year simulation, in agreement
485 with Theodorou et al. (2011). The spawning event occurred at the beginning of December
486 (Theodorou et al., 2011) and was illustrated by 12.6% tissue mass decline.

487

488 3.2 Microplastics accumulation and depuration phase

489

490 The hourly simulated MPs accumulation by the mussel in the North Sea and N. Ionian Sea are
491 shown in Fig. 6 and Fig. 7 respectively. In the North Sea, a 4-year-old wild mussel ($L=4.35$ cm,
492 $W=1.87$ g) contains 0.64 particles individual⁻¹ in August within the range value found by Van
493 Cauwenberghe et al. (2015) (0.4 ± 0.3 particles individual⁻¹). It is worth noting that Van
494 Cauwenberghe et al. (2015) allowed a 24 h clearance period, before analyzing mussels' tissue for
495 MPs, possibly resulting in slightly lower MPs accumulation than the model's prediction. In the N.
496 Ionian Sea, the simulated MPs accumulation by the cultured mussel with $L=4.88$ cm and $W=3.43$
497 g was 0.91 particles individual⁻¹ in July, in agreement with field observations obtained from Digka
498 et al. (2018a) (0.9 ± 0.2 particles individual⁻¹). In both regions, the model computed MPs
499 accumulation, assuming that the mussel treats MPs as silt particles (i.e. inedible particles) and is in
500 agreement with the available field data. This suggests that mussels probably present a common



501 behavior against all inedible particles. In model's results, based on the uptake and excretion rates of
502 MPs by the mussels in both study areas, the majority of MPs are rejected through pseudofaeces and
503 fewer through faeces production (not shown). This is in agreement with Woods et al. (2018) who
504 found that most microplastic fibers (71%) were quickly rejected as pseudofaeces and < 1% excreted
505 in faeces.

506 The small-scale fluctuations of MPs in the mussel (wild and cultivated) reflect the adopted
507 random variability of the environmental MPs concentration C_{env} and the daily environmental
508 forcing (CHL-a, temperature). The large-scale (seasonal) variability follows mainly the variability
509 of the clearance rate. The seasonal variability of the CHL-a concentration and temperature greatly
510 determines the variability of the clearance rate and hence the variability of MPs in the individual.
511 Moreover, the model predicts that mussel's energy needs are increased as it grows and therefore the
512 clearance rate is increased, resulting in higher MPs accumulation.

513 The simulated time needed to clean the mussel's gut from the MPs load for both areas is
514 shown in Fig. 8. In both areas, the cleaning follows an exponential decay, in agreement with Woods
515 et al. (2018). In particular, the model predicts a 90% mussel's cleaning after 330 hours (~14 days)
516 and 63 hours (~3 days) for the N. Ionian Sea and North Sea respectively. The cleaning process is
517 more rapid in the North Sea simulation, which can be attributed to the higher CHL-a concentration
518 found in this area, leading to increased production of faeces by the mussel and hence faster
519 excretion of the accumulated MPs. In the N. Ionian Sea, on the other hand, the rate of the mussel's
520 cleaning is slower, due to the limited food availability.

521

522 **3.3 Model's uncertainty regarding the environmental microplastics concentration**

523

524 The MPs concentration in the environment presents a strong variability in both temporal and
525 spatial scales. To examine the model's uncertainty related to the environmental MPs concentration
526 (C_{env}), a series of 15 and 13 simulations were performed in the North Sea and N. Ionian Sea
527 respectively, adopting different values of C_{env} within the observed range of each area. In the North
528 Sea, the adopted C_{env} ranged between 0.1 and 0.8 particles L^{-1} with a step of 0.05 (15 runs), while in
529 the N. Ionian Sea C_{env} ranged between 0.0012 and 0.0252 particles L^{-1} with a step of 0.002 (13
530 runs). The mean seasonal values and standard deviation of the 15 simulations in the North Sea and
531 the mean monthly values and standard deviation of the 13 simulations in the N. Ionian Sea were
532 computed and plotted in Fig. 9 and Fig. 10, respectively. Each error bar represents the uncertainty
533 of the simulated accumulation at the specific time, related to the environmental MPs concentration.

534 .



535 In both case studies, the uncertainty of the model appears to increase as the MPs accumulation
536 is increased. As the mussel grows in the North Sea, the mean value and standard deviation of MPs
537 accumulation is increased during the same season every year, illustrating the effect of the mussel's
538 weight. Moreover, the seasonal variability of the MPs accumulation should be caused by the
539 seasonality of CHL-a concentration. This is apparent during each year's spring: when CHL-a
540 concentration peaks at its maximum value ($\sim 30 \text{ mg m}^{-3}$; see Fig. 1), the filtration rate is decreased
541 (Riisgard et al., 2003, 2011), leading to lower MPs accumulation by the mussel and thus lower
542 model's uncertainty. In the N. Ionian Sea, the effect of the mussel's weight is more apparent in the
543 early months (~ 6 months), resulting on higher MPs accumulation and model uncertainty as the
544 mussel grows. Afterwards, the seasonality of both CHL-a concentration and temperature plays the
545 major role. During summer, when the CHL-a concentration is progressively decreased, reaching
546 minimum values ($\sim 0.7 \text{ mg /m}^3$) and temperature is increased ($>20^\circ \text{ C}$), the filtration rate is
547 significantly decreased or stopped, resulting in lower MPs accumulation and lower model's
548 uncertainty. This is in line with studies reporting that the mussel suspends the filtering activity and
549 thus closes its valves until better conditions occur (Pascoe et al., 2009, Riisgard et al., 2011).
550 Overall, the available field data lie within the model's uncertainty for both study areas.

551 Moreover, to evaluate the scenario adopted with the set-up of the previous experiments
552 (random C_{env} at a daily time step) 3 additional model runs are performed in each study area,
553 adopting each time different stochastic sequences of daily random C_{env} values within the observed
554 range, which is considered to reflect the high spatial and temporal variability of the environmental
555 MPs concentration. The mean value and standard deviation of these "stochastic" runs lie most of the
556 time within the standard deviation of the overall model's uncertainty in both case study areas (Fig. 9
557 and Fig. 10).

558

559 3.4 Sensitivity and Regression analysis results

560

561 The results of the sensitivity experiments regarding the MPs accumulation by the mussels are
562 shown in Fig. 11 and 12 for the North Sea and N. Ionian Sea respectively. The comparison between
563 the intertidal and subtidal mussel of the North Sea revealed that both +10% and -10% perturbation
564 of CHL-a and X_k have a slightly lower effect on the MPs accumulation by the intertidal mussel
565 which is probably attributed to the intermittent feeding periods experienced by the individual due to
566 the tide effect. As far as the temperature effect, both +10% and -10% perturbed value led to higher
567 sensitivity on the MPs accumulation by the intertidal mussel, due to the adopted modified
568 temperature relation during low tide. Especially, if the mussel's body temperature change during air



569 exposure would be considered, the perturbed temperature will probably affect even more the MPs
570 accumulation on the intertidal than the subtidal mussel. The effect of the C_{env} is slightly higher and
571 lower on the MPs accumulation by the intertidal mussel when perturbed +10% and -10%
572 respectively, however the difference of the sensitivity index (%) between the two mussels (intertidal
573 vs. subtidal) is small, indicating that the environmental MPs concentration affects similarly both
574 mussels, regardless the continuous or intermittent feeding-excretion process.

575 The comparison between the mussel sensitivity indexes in the N. Ionian and the North Sea
576 (in conditions of submergence) study areas reveals some important differences. Generally, most of
577 the perturbed (either +10% or -10%) variables and parameters (i.e. CHL-a, temperature, X_k) present
578 higher sensitivity on the MPs accumulation by the mussel from the N. Ionian Sea. This is attributed
579 to the prevailing environmental conditions and specifically the lower food availability (CHL-a) and
580 the higher temperature range in the N. Ionian Sea compared to the North Sea, which greatly
581 determine the feeding processes, the mussel's growth and hence the MPs accumulation. The
582 perturbed C_{env} in both study areas appears to affect similarly the MPs accumulation on both mussels
583 (-10%), with the small difference probably attributed to the higher abundance of seawater's MPs
584 present in the North Sea compared to the N. Ionian Sea. Finally, the half saturation coefficient for
585 the inorganic particles (Y_k) has no effect on the MPs accumulation of both North Sea and N. Ionian
586 Sea mussels, indicating that the amount of inedible particles (i.e. MPs) is relatively low in both
587 areas and thus the Y_k does not affect the way that the organic particles are being ingested
588 (Kooijman, 2006). According to Ren (2009), when the inorganic matter is low, the $K(y)$ (Eq. 5;
589 Table 1) is approximately equal to X_k and then Y_k is the least sensitive parameter for the ingestion
590 rate and thus growth.

591 The DEB-accumulation model output was used to determine the coefficients in Eq. 19 by the
592 nonlinear regression analysis: $b_1 = 0.1909 (\pm 0.0006)$, $b_2 = 0.0412 (\pm 0.0019)$, $b_3 = 0.1315 (\pm 0.00)$
593 and $b_4 = 1.1060 (\pm 0.0253)$. The confidence intervals for the estimated coefficients (b_1 , b_2 , b_3 , b_4) are
594 small enough which indicates an accurate estimation of them and the mean squared error of the
595 regression model is small enough (MSE=0.0523). Subsequently, as shown in Figure 13, Equation
596 20 may be used to predict the MPs concentration of the environment where mussels live, being in
597 most cases within the standard deviation of the field data. However, this is just a rough
598 demonstration of the method and should be implemented in more environments in order to be
599 further validated.

600

601



602 4. Discussion

603

604 A DEB-accumulation model was developed and validated with the only available data from
605 the North Sea and the N. Ionian Sea, to study the MPs accumulation by wild *M. edulis* and cultured
606 *M. galloprovincialis*, as they grow in different environments. Although the study is limited by
607 scarce validation data, it is notable that the accumulation submodel's parameters are extracted from
608 literature (Table 3) illustrating that mussels adopt a common defensive mechanism against inedible
609 particles (i.e. silt, MPs). Thus, the theoretical background constructed by Saraiva et al., (2011a)
610 (based on Kooijman, 2010) regarding the feeding and excretion processes of the mussel remains
611 unspoiled. Through the strong theoretical background of DEB theory, this study highlights that the
612 accumulation of MPs by the mussel is highly depended on the prevailing environmental conditions
613 which control the amount of MPs that the mussel filtrates and excretes.

614 Beginning with the generalization of the DEB model regarding the site-specific parameter
615 X_k in the N. Ionian Sea simulation, the function of the half saturation ($f(x) = a * [CHL - a]^b + c$)
616 successfully captures the physiological responses and thus the growth rate of the cultured mussel. In
617 the current study, a demonstration of this method is conducted leading to a DEB growth model
618 robust enough with a sufficiently generic nature for the simulation of the mussel growth in
619 representative mussel habitats of the Mediterranean Sea, covering a range of productivity and sea
620 surface temperature. Bourles et al. (2008) suggested for oyster growth (*Crassostrea gigas*) that a
621 seasonally varied half saturation coefficient could improve the accuracy of the food quantifier
622 because seawater composition is closely related to the season. As more field data becomes available
623 from various environments, such an approach could result to more generic formulations for the site-
624 specific parameter X_k , so that the model could be applied in several areas of interest, where field
625 growth data are absent and/or to simulate the potential mussel growth in the 2D space.

626 The simulation of MPs accumulation by the mussels, using the DEB-accumulation model, is
627 in good agreement with the available field data. The MPs accumulation by the cultivated mussel
628 (fresh tissue mass 3.42 g) originated from the N. Ionian Sea with mean $C_{env} = 0.0012 \pm 0.024$
629 particles L^{-1} , is 0.91 particles individual $^{-1}$ and by the wild mussel (fresh tissue mass 1.87 g) from the
630 North Sea with mean $C_{env} = 0.4 \pm 0.3$ particles L^{-1} is 0.64 particles individual $^{-1}$. If these
631 concentrations are expressed per gram of wet tissue of mussels, the cultivated mussel contamination
632 (0.27 particles $g^{-1}w.w.$) is comparable with the wild mussel (0.34 particles $g^{-1}w.w.$), despite the
633 much lower environmental MPs concentration (C_{env}) in the N. Ionian Sea than the North Sea. This
634 comparison aims to highlight the significant impact of the prevailing environmental conditions
635 (CHL-a and temperature) on the MPs accumulation by the mussels, although they originate from



636 different areas and lived different time period. The generally high abundance of CHL-a in the North
637 Sea simulation, contributes to a reduction of the filtering activity and hence of the MPs
638 accumulation. The threshold algal concentration for reduction of the mussel's filtration rate
639 (incipient saturation) has been found to lie between 6.3 and 10.0 $\mu\text{g chl a L}^{-1}$ (Riisgard et al., 2011),
640 which is the North Sea case. Furthermore, in the N. Ionian Sea simulation, the filtration, ingestion,
641 pseudofaeces and faeces production rates are decreased during the summer season when the CHL-a
642 and temperature has downward and upward trend respectively, gradually leading to a decline of the
643 mussel's MPs accumulation. Van Cauwenberghe and Janssen (2014) found that cultivated *M. edulis*
644 from the North Sea contained on average 0.36 ± 0.07 particles $\text{g}^{-1}\text{w.w.}$, a similar value with that
645 found in the present study for the wild mussel of the North Sea (0.34 particles $\text{g}^{-1}\text{w.w.}$). This
646 probably highlights the small contribution of mussel farms as a source of MPs pollution (Santana et
647 al., 2018). Moreover, the intertidal wild mussel (present study) is assumed to filter and excrete MPs
648 half of the time in comparison with the submerged cultured mussel in the North Sea, resulting
649 though in similar accumulation level. The model also predicts the time needed for the 90% gut
650 clearance of both cultured (N. Ionian Sea) and wild (North Sea) mussel to be almost 330 hours and
651 63 hours (equivalent to 14 and 3 days) respectively, when MPs contamination is removed from their
652 habitat. This is in line with a series of studies which demonstrated that the depuration time varies
653 between 6-72 hours and can last up to 40 days depending on several factors such as species,
654 environmental conditions (Bayne et al., 1987), size and type of MPs (Browne et al., 2008, Ward and
655 Kach, 2009, Woods et al., 2018, Birnstiel et al., 2019).

656 The strong dependence of food (CHL-a), temperature and seawater's MPs concentration on
657 the MPs accumulation by the mussel, regarding its wet weight, is demonstrated through sensitivity
658 experiments that were used to derive a rather simple nonlinear regression model (Eq. 19). The
659 comparison of the regression model's with the DEB model's output resulted in a quite accurate
660 estimation of the coefficients, which in turn sparked the idea of a 'new' relationship (Eq. 20) that
661 could potentially predict the MPs concentration in the environment when certain conditions are
662 known (CHL-a, T, C_{env} , W). The latter equation was applied in 8 areas in total (2 from the present
663 study areas and 6 from Li et al. (2018), with relatively good results since the predicted value is
664 within the observed range of field data in most regions, making the mussel a potential bioindicator.
665 Mussels have been previously proposed as bioindicators for marine microplastic pollution (<1 mm),
666 although the efficient gut clearance and selective feeding behavior limit their quantitative ability
667 (Lusher et al., 2017, Brate et al., 2018, Beyer et al., 2017, Fossi et al., 2018, Li et al., 2019). The
668 very recent study by Ward et al. (2019) demonstrated that bivalves are poor bioindicators of MPs
669 pollution due to the particle selection during feeding and excretion processes that is based on the
670 physical characteristics of the MPs. Considering that the MPs accumulation is site-dependent and



671 that sampling of mussels is usually easier than seawater (Karlsson et al., 2017, Brate et al., 2018),
672 models like the one described in Eq. 20 that besides the MPs accumulation take into account
673 characteristics of the environment, which are crucial for the way that mussels accumulate MPs,
674 possibly could be used at global level and allow comparisons between various environments.
675 However, the method described should be validated in more environments with more frequent field
676 data to be able to provide secure results.

677 Despite the scarce validation data, in this study there are some other limitations. First of all,
678 the data regarding the concentration of MPs in the mussels' environment is also scarce; since MPs
679 is a relatively recent subject of study, the existing knowledge of the spatial and temporal
680 distribution is still quite limited (Law and Thompson, 2014, Browne, 2015, Anderson et al., 2016,
681 de Sa et al., 2018, Smith et al., 2018, Troost et al., 2018). To overcome the lack of environmental
682 MPs time series, a function of randomly generated values within the observed range of each area
683 was applied and its uncertainty was examined through an ensemble forecasting. Specifically, the
684 model's uncertainty due to the environmental MPs concentration (C_{env}) was tested by performing a
685 series of model runs forced by an envelope of representative values of C_{env} and the results (section
686 3.3) show that the adopted stochastic scenario simulates realistically the MPs accumulation by the
687 mussels and in agreement with the available field data. The approach used is assumed to be close to
688 reality since it has been reported that MPs quantification in the water is rather a complicated
689 procedure due to the influence of many factors such as tides, wind, wave action, ocean currents,
690 river inputs and hydrodynamic features resulting to high spatially and temporally variability of MPs
691 distribution even in very small scales (Messinetti et al., 2018, Goldstein et al., 2013). In a future
692 work the DEB-accumulation model could be coupled with a high-resolution MPs distribution model
693 (Kalaroni et al., 2019) to overcome this limitation. Moreover, the approach followed in calculating
694 the value of MPs concentration in the near surface layer (0-5m depth) (Kooi et al., 2016), resulted in
695 a representative value of the upper ocean layer. In depth knowledge of the MPs distribution, both
696 horizontally and vertically, is essential to understand and mitigate their impact not only on the
697 various marine compartments but also on the organisms inhabiting those (Van Sebille et al., 2015,
698 Kooi et al., 2016). For that reason, it is important to enhance the monitoring activity especially in
699 the vulnerable coastal environments, adopting integrated cross-disciplinary approaches and
700 monitoring of biological, physical and chemical parameters which provide information on the
701 ecosystem function, in order to improve the assessment of emerging pollutants (i.e. MPs) and their
702 impacts on biota (objective of JERICO-RI framework).

703 Further, the assumption that the mussel has the same filtration rate for all particles
704 independently of their chemical composition, size and shape, is a simplification and a contradictory
705 theme of discussion (see Saraiva et al., 2011a for details). However, through the model, a pre-



706 ingestive particle selection by the mussel is implied based on the organic-inorganic content of the
707 suspended matter illustrating the different binding probabilities applied for algal and MPs particles
708 during the ingestion process. Through an investigation of wild mussel's faeces and pseudofaeces
709 production in laboratory conditions, Zhao et al. (2018) found that the length of MPs was
710 significantly longer in pseudofaeces than in the digestive gland and faeces. Furthermore, Van
711 Cauwenberghe et al. (2015) demonstrated that mussel's faeces contained larger MPs (15–500 μm)
712 compared to the mussel's tissue (20–90 μm). Apparently, smaller sized MPs seem to be dominant
713 within the mussels in comparison with the ambient environment (Li et al., 2018, Qu et al., 2018,
714 Digka et al., 2018b), implying that the mussel is more prone to ingest and retain smaller sized MPs.
715 As an example, Digka et al. (2018b) confirmed that the smaller MPs (<1 mm) occupy the 62.3%,
716 96.9% and 100% in seawater, sediments and mussels from the N. Ionian Sea respectively. In a
717 future work this selection pattern regarding size, could be simulated by suitable preference weights
718 among different MPs sizes. This will improve the knowledge of the feeding and excretion
719 mechanisms used by the mussels against MPs pollution and the assessment of the ecological
720 footprint (Rist et al., 2019).

721 Moreover, the assumption that the contamination by MPs does not affect the energy budget
722 in terms of growth might also be a simplification as this is a subject currently under investigation.
723 Van Cauwenberghe et al. (2015) found that although mussels *M. edulis* exposed to MPs increased
724 their energy consumption, the energy reserves was not affected compared to the control organisms,
725 implying that mussels are able to adopt a defensive mechanism against the suspended inorganic
726 particles (i.e. MPs) (Ward and Shumway, 2004). Furthermore, MPs exposure showed no significant
727 effect on mussel's *Perna perna* energy budget, despite its long duration and relatively realistic
728 intensity, concluding to the assumption of mussel's acclimation to maintain its health (Santana et
729 al., 2018). On the contrary, other authors who mainly intended to predict future effects, suggested a
730 significant energy shift from reproduction to structural growth and elevated maintenance costs,
731 probably attributed to the reduced energy intake, when the organisms (i.e. oyster *Crassostrea gigas*)
732 were contaminated with high and unrealistic concentration of MPs (Sussarellu et al., 2016).
733 Moreover, Gardon et al. (2018) showed that the overall energy balance of oyster *Pinctada*
734 *margaritifera* was significantly impacted by the reduced assimilation efficiency in correlation with
735 the exposed dose of MPs and for that reason energy had to be withdrawn from reproduction to
736 compensate for the energy loss. In future dedicated experiments exploring the effects on all
737 components of a DEB model should be carried out considering long-term realistic MPs exposure.

738 Furthermore, the tide data as considered in the present study impose model's bias, since the
739 mussel's body temperature change when exposed to air was not taken into consideration. Assessing
740 mussel's body temperature demand extended experiments in field conditions (Tagliarolo and



741 McQuaid, 2015, Monaco and McQuaid, 2018). A very recent study by Seuront et al. (2019) along
742 the French coast of the eastern English Channel found no significant correlation between air's and
743 mussel's body temperature but rather positively significant correlation with the hard substrate's (i.e.
744 rocks) temperature. However, in the present study the tide effect on processes that are affected by
745 the thermal equation ($k(T)$) is considered through the metabolic depression (details in section 2.4).
746 Sara et al. (2011) following the method developed by Kearney et al. (2010), who coupled a DEB
747 model with a biophysical model, incorporated the change of mussel's body temperature during
748 emersion, using information of various climatological variables (i.e. solar radiation, air temperature,
749 wind speed, wave height), but the temperature sensitivity on the physiological processes was
750 ignored. In a future study, a similar approach by coupling the present DEB-accumulation model
751 with a biophysical model could be followed and lead to a more detailed simulation of the mussel's
752 body temperature.

753 5. Conclusions

754

755 In a future study the model should be validated against more frequent field data regarding
756 the MPs accumulation, with sampling of mussels among various sizes and life stages as for now it
757 cannot be reliable in conducting predictions within accepted precision. However, this study
758 provides a new approach in studying the accumulation of MPs by filter feeders and reveals the
759 relations between characteristics of the mussel's surrounding environment and the MPs
760 accumulation, which is presented with high seasonal fluctuations. Additionally, in a future study the
761 DEB-accumulation model will be coupled with a coupled hydrodynamic-biochemical model
762 (Petihakis et al., 2002, 2012, Triantafyllou et al., 2003, Tsiaras et al., 2014, Ciavatta et al., 2019,
763 Kalaroni et al., 2020) and a MPs distribution model (Kalaroni et al., 2019) that will provide fields of
764 temperature, food availability and MPs concentration respectively at the Mediterranean scale, and
765 eventually lead to an integrated representation of the MPs accumulation by mussels (Daewel et al.,
766 2008). This fully coupled model will be downscaled to the Cretan Sea SuperSite, while the
767 parameterization of important biological processes will be redesigned based on the new data which
768 will be acquired in the framework of the JERICO S3 project (<http://www.jerico-ri.eu>). The present
769 study highlights the urgent need for adopting a multi-disciplinary monitoring activity by measuring
770 physical, biological and chemical parameters that are crucial for mapping the MPs distribution,
771 assessing the contamination level of the marine organisms and investigating the impact on the
772 health status. Overall, despite the significant limitations that were mentioned before, taken into
773 account that plastics are one of the global hot issues, this particular study could help for the design
774 of next efforts, since it provides indications on the future priority related issues.



775

776 **Author Contribution:**

777 **Natalia Stamataki, Yannis Hatzonikolakis, Kostas Tsiaras, Catherine Tsangaris, George**
778 **Petihakis, Sarantis Sofianos, George Triantafyllou**

779

780 G.T. conceived the basic idea of the present study and was responsible for the management and
781 coordination of the research planning and execution. N.S. and Y.H. developed the model code with
782 the contribution of K.T.. N.S. collected the existing information on the subject and performed the
783 simulations of the present study with the help of Y.H. when needed. G.T., G.P., K.T., Y.H. and N.S.
784 contributed to the interpretation of the results. C.T. provided the field data of the mussel's
785 microplastic accumulation in the North Ionian Sea. N.S. prepared the manuscript, with critical
786 review, commentary and revision contributed from all co-authors.

787

788 **Competing interests:**

789 The authors declare that they have no conflict of interest.

790

791 **Acknowledgments:**

792

793 This work was partially funded by the national project 'Blue growth with innovation and
794 application in Greek Seas' (MIS 5002438) and the EU H2020 CLAIM project (G.A. n° 774586).
795 This study has been conducted using E.U. Copernicus Marine Service Information
796 (<http://marine.copernicus.eu/>). Part of this work was supported by the JERICO- NEXT project. This
797 project has received funding from the European Union's Horizon 2020
798 research and innovation programme under grant agreement no. 654410.

799

800

801

802

803



804 References

- 805 Alunno-Bruscia, M., Bourlès, Y., Maurer, D., Robert, S., Mazurié, J., Gangnery, A., Gouilletquer, P. and
806 Pouvreau, S.: A single bio-energetics growth and reproduction model for the oyster *Crassostrea gigas* in six Atlantic
807 ecosystems, *J. Sea Res.*, 66(4), 340–348, doi:10.1016/j.seares.2011.07.008, 2011.
- 808 Anderson, J. C., Park, B. J. and Palace, V. P.: Microplastics in aquatic environments: Implications for Canadian
809 ecosystems, *Environ. Pollut.*, 218, 269–280, doi:10.1016/j.envpol.2016.06.074, 2016.
- 810 Andrady, A. L.: Microplastics in the marine environment, *Mar. Pollut. Bull.*, 62(8), 1596–1605,
811 doi:10.1016/j.marpolbul.2011.05.030, 2011.
- 812 Arthur, C., J. Baker and H. Bamford (eds). Proceedings of the International Research Workshop on the
813 Occurrence, Effects and Fate of Microplastic Marine Debris. Sept 9–11, 2008. NOAA Technical Memorandum NOS-
814 OR&R-30, 2009
- 815 Bacher, C. and Gangnery, A.: Use of dynamic energy budget and individual based models to simulate the
816 dynamics of cultivated oyster populations, *J. Sea Res.*, 56(2), 140–155, doi:10.1016/j.seares.2006.03.004, 2006.
- 817 Bayne, B. and Worrall, C.: Growth and Production of Mussels *Mytilus edulis* from Two Populations, *Mar. Ecol.*
818 *Prog. Ser.*, 3, 317–328, doi:10.3354/meps003317, 1980.
- 819 Bayne, B. L., Hawkins, A. J. S. and Navarro, E.: Feeding and digestion by the mussel *Mytilus edulis* L.
820 (*Bivalvia*: *Mollusca*) in mixtures of silt and algal cells at low concentrations, *J. Exp. Mar. Bio. Ecol.*, 111(1), 1–22,
821 doi:10.1016/0022-0981(87)90017-7, 1987.
- 822 Béjaoui-Omri, A., Béjaoui, B., Harzallah, A., Aloui-Béjaoui, N., El Bour, M. and Aleya, L.: Dynamic energy
823 budget model: a monitoring tool for growth and reproduction performance of *Mytilus galloprovincialis* in Bizerte
824 Lagoon (Southwestern Mediterranean Sea), *Environ. Sci. Pollut. Res.*, 21(22), 13081–13094, doi:10.1007/s11356-014-
825 3265-1, 2014.
- 826 Beyer, J., Green, N. W., Brooks, S., Allan, I. J., Ruus, A., Gomes, T., Bråte, I. L. N. and Schøyen, M.: Blue
827 mussels (*Mytilus edulis* spp.) as sentinel organisms in coastal pollution monitoring: A review, *Mar. Environ. Res.*,
828 130, 338–365, doi:10.1016/j.marenvres.2017.07.024, 2017.
- 829 Birnstiel, S., Soares-Gomes, A. and da Gama, B. A. P.: Depuration reduces microplastic content in wild and
830 farmed mussels, *Mar. Pollut. Bull.*, 140, 241–247, doi:10.1016/j.marpolbul.2019.01.044, 2019.
- 831 Bourlès, Y., Alunno-Bruscia, M., Pouvreau, S., Tollu, G., Leguay, D., Arnaud, C., Gouilletquer, P. and
832 Kooijman, S. A. L. M.: Modelling growth and reproduction of the Pacific oyster *Crassostrea gigas*: Advances in the
833 oyster-DEB model through application to a coastal pond, *J. Sea Res.*, 62(2–3), 62–71,
834 doi:10.1016/j.seares.2009.03.002, 2009.
- 835 Bråte, I. L. N., Hurley, R., Iversen, K., Beyer, J., Thomas, K. V., Steindal, C. C., Green, N. W., Olsen, M. and
836 Lusher, A.: *Mytilus* spp. as sentinels for monitoring microplastic pollution in Norwegian coastal waters: A qualitative
837 and quantitative study, *Environ. Pollut.*, 243, 383–393, doi:10.1016/j.envpol.2018.08.077, 2018.
- 838 Browne, M. A., Dissanayake, A., Galloway, T. S., Lowe, D. M. and Thompson, R. C.: Ingested microscopic
839 plastic translocates to the circulatory system of the mussel, *Mytilus edulis* (L.), *Environ. Sci. Technol.*, 42(13), 5026–
840 5031, doi:10.1021/es800249a, 2008.
- 841 Browne, M. A., Galloway, T. and Thompson, R.: Microplastic—an emerging contaminant of potential concern?,
842 *Integr. Environ. Assess. Manag.*, 3(4), 559–561, doi:10.1002/ieam.5630030412, 2007.
- 843 Browne, M. A.: Sources and pathways of microplastics to habitats, *Mar. Anthropog. Litter*, 229–244,
844 doi:10.1007/978-3-319-16510-3_9, 2015.
- 845 Capolupo, M., Franzellitti, S., Valbonesi, P., Lanzas, C. S. and Fabbri, E.: Uptake and transcriptional effects of
846 polystyrene microplastics in larval stages of the Mediterranean mussel *Mytilus galloprovincialis*, *Environ. Pollut.*, 241,
847 1038–1047, doi:10.1016/j.envpol.2018.06.035, 2018.
- 848 Cardoso, J. F. M. F., Dekker, R., Witte, J. I. J. and van der Veer, H. W.: Is reproductive failure responsible for
849 reduced recruitment of intertidal *Mytilus edulis* L. in the western Dutch Wadden Sea?, *Senckenbergiana Maritima*,
850 37(2), 83–92, doi:10.1007/BF03043695, 2007.
- 851 Casas, S. and Bacher, C.: Modelling trace metal (Hg and Pb) bioaccumulation in the Mediterranean mussel,
852 *Mytilus galloprovincialis*, applied to environmental monitoring, *J. Sea Res.*, 56(2), 168–181,
853 doi:10.1016/j.seares.2006.03.006, 2006.
- 854 Ciavatta, S., Kay, S., Brewin, R. J. W., Cox, R., Di Cicco, A., Nencioli, F., Polimene, L., Sammartino, M.,
855 Santoleri, R., Skákala, J. and Tsapakis, M.: Ecoregions in the Mediterranean Sea Through the Reanalysis of



- 856 Phytoplankton Functional Types and Carbon Fluxes, *J. Geophys. Res. Ocean.*, 124(10), 6737–6759,
857 doi:10.1029/2019JC015128, 2019.
- 858 Cole, M., Lindeque, P., Fileman, E., Halsband, C., Goodhead, R., Moger, J. and Galloway, T. S.: Microplastic
859 ingestion by zooplankton, *Environ. Sci. Technol.*, 47(12), 6646–6655, doi:10.1021/es400663f, 2013.
- 860 Cole, M., Lindeque, P., Halsband, C. and Galloway, T. S.: Microplastics as contaminants in the marine
861 environment: A review, *Mar. Pollut. Bull.*, 62(12), 2588–2597, doi:10.1016/j.marpolbul.2011.09.025, 2011.
- 862 Cucci, T. L., Shumway, S. E., Brown, W. S. and Newell, C. R.: Using phytoplankton and flow cytometry to
863 analyze grazing by marine organisms, *Cytometry*, 10(5), 659–669, doi:10.1002/cyto.990100523, 1989.
- 864 Daewel, U., Peck, M. A., Kühn, W., St. John, M. A., Alekseeva, I. and Schrum, C.: Coupling ecosystem and
865 individual-based models to simulate the influence of environmental variability on potential growth and survival of
866 larval sprat (*Sprattus sprattus* L.) in the North Sea, *Fish. Oceanogr.*, 17(5), 333–351, doi:10.1111/j.1365-
867 2419.2008.00482.x, 2008.
- 868 de Sá, L. C., Oliveira, M., Ribeiro, F., Rocha, T. L. and Futter, M. N.: Studies of the effects of microplastics on
869 aquatic organisms: What do we know and where should we focus our efforts in the future?, *Sci. Total Environ.*, 645,
870 1029–1039, doi:10.1016/j.scitotenv.2018.07.207, 2018.
- 871 De Witte, B., Devriese, L., Bekaert, K., Hoffman, S., Vandermeersch, G., Cooreman, K. and Robbens, J.: Quality
872 assessment of the blue mussel (*Mytilus edulis*): Comparison between commercial and wild types, *Mar. Pollut. Bull.*,
873 85(1), 146–155, doi:10.1016/j.marpolbul.2014.06.006, 2014.
- 874 Digka, N., Tsangaris, C., Kaberi, H., Adamopoulou, A. and Zeri, C.: Microplastic Abundance and Polymer
875 Types in a Mediterranean Environment, *Springer Water.*, 2018b.
- 876 Digka, N., Tsangaris, C., Torre, M., Anastasopoulou, A. and Zeri, C.: Microplastics in mussels and fish from the
877 Northern Ionian Sea, *Mar. Pollut. Bull.*, 135, 30–40, doi:10.1016/j.marpolbul.2018.06.063, 2018a.
- 878 Enders, K., Lenz, R., Stedmon, C. A. and Nielsen, T. G.: Abundance, size and polymer composition of marine
879 microplastics $\geq 10 \mu\text{m}$ in the Atlantic Ocean and their modelled vertical distribution, *Mar. Pollut. Bull.*, 100(1), 70–81,
880 doi:10.1016/j.marpolbul.2015.09.027, 2015.
- 881 Eriksen, M., Lebreton, L. C. M., Carson, H. S., Thiel, M., Moore, C. J., Borerro, J. C., Galgani, F., Ryan, P. G.
882 and Reisser, J.: Plastic Pollution in the World's Oceans: More than 5 Trillion Plastic Pieces Weighing over 250,000
883 Tons Afloat at Sea, *PLoS One*, 9(12), doi:10.1371/journal.pone.0111913, 2014.
- 884 Everaert, G., Van Cauwenberghe, L., De Rijcke, M., Koelmans, A. A., Mees, J., Vandegehuchte, M. and Janssen,
885 C. R.: Risk assessment of microplastics in the ocean: Modelling approach and first conclusions, *Environ. Pollut.*, 242,
886 1930–1938, doi:10.1016/j.envpol.2018.07.069, 2018.
- 887 Fossi, M. C., Pedà, C., Compa, M., Tsangaris, C., Alomar, C., Claro, F., Ioakeimidis, C., Galgani, F., Hema, T.,
888 Deudero, S., Romeo, T., Battaglia, P., Andaloro, F., Caliani, I., Casini, S., Panti, C. and Baini, M.: Bioindicators for
889 monitoring marine litter ingestion and its impacts on Mediterranean biodiversity, *Environ. Pollut.*, 237, 1023–1040,
890 doi:10.1016/j.envpol.2017.11.019, 2018.
- 891 Gardon, T., Reisser, C., Soyeux, C., Quillien, V. and Le Moullac, G.: Microplastics Affect Energy Balance and
892 Gametogenesis in the Pearl Oyster *Pinctada margaritifera*, *Environ. Sci. Technol.*, 52(9), 5277–5286,
893 doi:10.1021/acs.est.8b00168, 2018.
- 894 GESAMP Joint Group of Experts on the Scientific Aspects of Marine Environmental Protection: Sources, fate
895 and effects of microplastics in the marine environment: a global assessment”, edited by P. J. Kershaw and ed), *Reports*
896 *Stud. GESAMP*, 90(90), 96, doi:10.13140/RG.2.1.3803.7925, 2015.
- 897 *GlobColour data* (<http://globcolour.info>) used in this study has been developed, validated, and distributed by
898 *ACRI-ST, France*.
- 899 Gohin, F., Druon, J. N. and Lampert, L.: A five channel chlorophyll concentration algorithm applied to Sea
900 WiFS data processed by SeaDAS in coastal waters, *Int. J. Remote Sens.*, 23(8), 1639–1661,
901 doi:10.1080/01431160110071879, 2002.
- 902 Goldstein, M. C., Titmus, A. J. and Ford, M.: Scales of spatial heterogeneity of plastic marine debris in the
903 northeast Pacific Ocean, *PLoS One*, 8(11), 80020, doi:10.1371/journal.pone.0080020, 2013.
- 904 Handå, A., Alver, M., Edvardsen, C. V., Halstensen, S., Olsen, A. J., Øie, G., Reitan, K. I., Olsen, Y. and
905 Reinertsen, H.: Growth of farmed blue mussels (*Mytilus edulis* L.) in a Norwegian coastal area; comparison of food
906 proxies by DEB modeling, *J. Sea Res.*, 66(4), 297–307, doi:10.1016/j.seares.2011.05.005, 2011.
- 907 Hantoro, I., Löhr, A. J., Van Belleghem, F. G. A. J., Widanarko, B. and Ragas, A. M. J.: Microplastics in coastal
908 areas and seafood: implications for food safety, *Food Addit. Contam. - Part A Chem. Anal. Control. Expo. Risk*
909 *Assess.*, 36(5), 674–711, doi:10.1080/19440049.2019.1585581, 2019.



- 910 Hatzonikolakis, Y., Tsiaras, K., Theodorou, J. A., Petihakis, G., Sofianos, S. and Triantafyllou, G.: Simulation of
911 mussel *Mytilus galloprovincialis* growth with a dynamic energy budget model in Maliakos and Thermaikos Gulfs
912 (Eastern Mediterranean), *Aquac. Environ. Interact.*, 9, 371–383, doi:10.3354/aei00236, 2017.
- 913 Hirai, H., Takada, H., Ogata, Y., Yamashita, R., Mizukawa, K., Saha, M., Kwan, C., Moore, C., Gray, H.,
914 Laursen, D., Zettler, E. R., Farrington, J. W., Reddy, C. M., Peacock, E. E. and Ward, M. W.: Organic micropollutants
915 in marine plastics debris from the open ocean and remote and urban beaches, *Mar. Pollut. Bull.*, 62(8), 1683–1692,
916 doi:10.1016/j.marpolbul.2011.06.004, 2011.
- 917 Jacobs, P., Beauchemin, C. and Riegman, R.: Growth of juvenile blue mussels (*Mytilus edulis*) on suspended
918 collectors in the Dutch Wadden Sea, *J. Sea Res.*, 85, 365–371, doi:10.1016/j.seares.2013.07.006, 2014.
- 919 Jacobs, P., Troost, K., Riegman, R. and van der Meer, J.: Length- and weight-dependent clearance rates of
920 juvenile mussels (*Mytilus edulis*) on various planktonic prey items, *Helgol. Mar. Res.*, 69(1), 101–112,
921 doi:10.1007/s10152-014-0419-y, 2015.
- 922 Jolliff, J. K., Kindle, J. C., Shulman, I., Penta, B., Friedrichs, M. A. M., Helber, R. and Arnone, R. A.: Summary
923 diagrams for coupled hydrodynamic-ecosystem model skill assessment, *J. Mar. Syst.*, 76(1–2), 64–82,
924 doi:10.1016/j.jmarsys.2008.05.014, 2009.
- 925 Jørgensen, C., Larsen, P. and Riisgård, H.: Effects of temperature on the mussel pump, *Mar. Ecol. Prog. Ser.*,
926 64(1/2), 89–97, doi:10.3354/meps064089, 1990.
- 927 Kalaroni S, Hatzonikolakis Y, Tsiaras K, Gkanasos A, Triantafyllou G.: Modelling the Marine Microplastic
928 Distribution from Municipal Wastewater in Saronikos Gulf (E. Mediterranean). *Oceanogr Fish Open Access J.*; 9(1):
929 555752. DOI: 10.19080/OFOAJ.2019.09.555752, 2019.
- 930 Kalaroni, S., Tsiaras, K., Petihakis, G., Economou-Amilli, A. and Triantafyllou, G.: Modelling the
931 Mediterranean pelagic ecosystem using the POSEIDON ecological model. Part I: Nutrients and chlorophyll-a
932 dynamics, *Deep. Res. Part II Top. Stud. Oceanogr.*, 171, 104647, doi:10.1016/j.dsr2.2019.104647, 2020.
- 933 Karayücel, S., Çelik, M. Y., Karayücel, I. and Erik, G.: Karadeniz’de Sinop İlinde Akdeniz Midyesinin (*Mytilus*
934 *galloprovincialis* Lamarck, 1819) Sal Sisteminde Büyümesi ve Üretimi, *Turkish J. Fish. Aquat. Sci.*, 10(1), 9–17,
935 doi:10.4194/trjfas.2010.0102, 2010.
- 936 Karlsson, T. M., Vethaak, A. D., Almroth, B. C., Ariese, F., van Velzen, M., Hasselöv, M. and Leslie, H. A.:
937 Screening for microplastics in sediment, water, marine invertebrates and fish: Method development and microplastic
938 accumulation, *Mar. Pollut. Bull.*, 122(1–2), 403–408, doi:10.1016/j.marpolbul.2017.06.081, 2017.
- 939 Kearney, M., Simpson, S. J., Raubenheimer, D. and Helmuth, B.: Modelling the ecological niche from functional
940 traits, *Philos. Trans. R. Soc. B Biol. Sci.*, 365(1557), 3469–3483, doi:10.1098/rstb.2010.0034, 2010.
- 941 Khan, M. B. and Prezant, R. S.: Microplastic abundances in a mussel bed and ingestion by the ribbed marsh
942 mussel *Geukensia demissa*, *Mar. Pollut. Bull.*, 130, 67–75, doi:10.1016/j.marpolbul.2018.03.012, 2018.
- 943 Kiørboe, T. and Møhlenberg, F.: Particle Selection in Suspension-Feeding Bivalves, *Mar. Ecol. Prog. Ser.*, 5,
944 291–296, doi:10.3354/meps005291, 1981.
- 945 Kooi, M., Reisser, J., Slat, B., Ferrari, F. F., Schmid, M. S., Cunsolo, S., Brambini, R., Noble, K., Sirks, L. A.,
946 Linders, T. E. W., Schoeneich-Argent, R. I. and Koelmans, A. A.: The effect of particle properties on the depth profile
947 of buoyant plastics in the ocean, *Sci. Rep.*, 6(1), doi:10.1038/srep33882, 2016.
- 948 Kooijman SALM: *Dynamic Energy Budget Theory for Metabolic Organisation*. Cambridge University Press,
949 Cambridge, 2010.
- 950 Kooijman, S. A. L. M.: *Dynamic Energy and Mass Budgets in Biological Systems*. Cambridge: Cambridge
951 University Press, 2000.
- 952 Kooijman, S. A. L. M.: Pseudo-faeces production in bivalves, *J. Sea Res.*, 56(2), 103–106,
953 doi:10.1016/j.seares.2006.03.003, 2006.
- 954 Lacroix, G., Ruddick, K., Ozer, J. and Lancelot, C.: Modelling the impact of the Scheldt and Rhine/Meuse
955 plumes on the salinity distribution in Belgian waters (southern North Sea), *J. Sea Res.*, 52(3), 149–163,
956 doi:10.1016/j.seares.2004.01.003, 2004.
- 957 Lattin, G. L., Moore, C. J., Zellers, A. F., Moore, S. L. and Weisberg, S. B.: A comparison of neustonic plastic
958 and zooplankton at different depths near the southern California shore, *Mar. Pollut. Bull.*, 49(4), 291–294,
959 doi:10.1016/j.marpolbul.2004.01.020, 2004.
- 960 Law, K. L. and Thompson, R. C.: Microplastics in the seas, *Science (80-.)*, 345(6193), 144–145,
961 doi:10.1126/science.1254065, 2014.
- 962 Lenz, R., Enders, K. and Nielsen, T. G.: Microplastic exposure studies should be environmentally realistic, *Proc.*
963 *Natl. Acad. Sci. U. S. A.*, 113(29), E4121–E4122, doi:10.1073/pnas.1606615113, 2016.



- 964 Li, J., Green, C., Reynolds, A., Shi, H. and Rotchell, J. M.: Microplastics in mussels sampled from coastal waters
965 and supermarkets in the United Kingdom, *Environ. Pollut.*, 241, 35–44, doi:10.1016/j.envpol.2018.05.038, 2018.
- 966 Li, J., Lusher, A. L., Rotchell, J. M., Deudero, S., Turra, A., Bråte, I. L. N., Sun, C., Shahadat Hossain, M., Li,
967 Q., Kolandhasamy, P. and Shi, H.: Using mussel as a global bioindicator of coastal microplastic pollution, *Environ.*
968 *Pollut.*, 244, 522–533, doi:10.1016/j.envpol.2018.10.032, 2019.
- 969 Li, J., Qu, X., Su, L., Zhang, W., Yang, D., Kolandhasamy, P., Li, D. and Shi, H.: Microplastics in mussels along
970 the coastal waters of China, *Environ. Pollut.*, 214, 177–184, doi:10.1016/j.envpol.2016.04.012, 2016.
- 971 Liubartseva, S., Coppini, G., Lecci, R. and Clementi, E.: Tracking plastics in the Mediterranean: 2D Lagrangian
972 model, *Mar. Pollut. Bull.*, 129(1), 151–162, doi:10.1016/j.marpolbul.2018.02.019, 2018.
- 973 Lusher, A., Bråte, I. L. N., Hurley, R., Iversen, K. and Olsen, M.: Testing of methodology for measuring
974 microplastics in blue mussels (*Mytilus* spp) and sediments, and recommendations for future monitoring of
975 microplastics, 87, (7209), doi:10.13140/RG.2.2.24399.59041, 2017.
- 976 Lusher, A.: Microplastics in the marine environment: Distribution, interactions and effects, *Mar. Anthropog.*
977 *Litter*, 245–307, doi:10.1007/978-3-319-16510-3_10, 2015.
- 978 Maes, T., Van der Meulen, M. D., Devriese, L. I., Leslie, H. A., Huvet, A., Frère, L., Robbens, J. and Vethaak,
979 A. D.: Microplastics baseline surveys at the water surface and in sediments of the North-East Atlantic, *Front. Mar.*
980 *Sci.*, 4(MAY), doi:10.3389/fmars.2017.00135, 2017.
- 981 Maire, O., Amouroux, J. M., Duchêne, J. C. and Grémare, A.: Relationship between filtration activity and food
982 availability in the Mediterranean mussel *Mytilus galloprovincialis*, *Mar. Biol.*, 152(6), 1293–1307,
983 doi:10.1007/s00227-007-0778-x, 2007.
- 984 MarLIN: The Marine Life Information Network - Common mussel (*Mytilus edulis*). Available from:
985 <https://www.marlin.ac.uk/species/detail/1421>, 2016.
- 986 Mathalon, A. and Hill, P.: Microplastic fibers in the intertidal ecosystem surrounding Halifax Harbor, Nova
987 Scotia, *Mar. Pollut. Bull.*, 81(1), 69–79, doi:10.1016/j.marpolbul.2014.02.018, 2014.
- 988 Mato, Y., Isobe, T., Takada, H., Kanehiro, H., Ohtake, C. and Kaminuma, T.: Plastic resin pellets as a transport
989 medium for toxic chemicals in the marine environment, *Environ. Sci. Technol.*, 35(2), 318–324,
990 doi:10.1021/es0010498, 2001.
- 991 Messinetti, S., Mercurio, S., Parolini, M., Sugni, M. and Pennati, R.: Effects of polystyrene microplastics on
992 early stages of two marine invertebrates with different feeding strategies, *Environ. Pollut.*, 237, 1080–1087,
993 doi:10.1016/j.envpol.2017.11.030, 2018.
- 994 Monaco, C. J. and McQuaid, C. D.: Applicability of Dynamic Energy Budget (DEB) models across steep
995 environmental gradients, *Sci. Rep.*, 8(1), doi:10.1038/s41598-018-34786-w, 2018.
- 996 Moore, C. J., Moore, S. L., Leecaster, M. K. and Weisberg, S. B.: A comparison of plastic and plankton in the
997 North Pacific Central Gyre, *Mar. Pollut. Bull.*, 42(12), 1297–1300, doi:10.1016/S0025-326X(01)00114-X, 2001.
- 998 Otto, L., Zimmerman, J. T. F., Furnes, G. K., Mork, M., Saetre, R. and Becker, G.: Review of the physical
999 oceanography of the North Sea, *Netherlands J. Sea Res.*, 26(2–4), 161, doi:10.1016/0077-7579(90)90091-T, 1990.
- 1000 Painting, S. J., Collingridge, K. A., Durand, D., Grémare, A., Créach, V., Arvanitidis, C. and Bernard, G.:
1001 Marine monitoring in Europe: is it adequate to address environmental threats and pressures?, *Ocean Sci. Discuss.*,
1002 16(1), 1–31, doi:10.5194/os-2019-75, 2019.
- 1003 Palacz, A. P., St. John, M. A., Brewin, R. J. W., Hirata, T. and Gregg, W. W.: Distribution of phytoplankton
1004 functional types in high-nitrate, low-chlorophyll waters in a new diagnostic ecological indicator model,
1005 *Biogeosciences*, 10(11), 7553–7574, doi:10.5194/bg-10-7553-2013, 2013.
- 1006 Pascoe, P. L., Parry, H. E. and Hawkins, A. J. S.: Observations on the measurement and interpretation of
1007 clearance rate variations in suspension-feeding bivalve shellfish, *Aquat. Biol.*, 6(1–3), 181–190, doi:10.3354/ab00123,
1008 2009.
- 1009 Pasquini, G., Ronchi, F., Strafella, P., Scarcella, G. and Fortibuoni, T.: Seabed litter composition, distribution
1010 and sources in the Northern and Central Adriatic Sea (Mediterranean), *Waste Manag.*, 58, 41–51,
1011 doi:10.1016/j.wasman.2016.08.038, 2016.
- 1012 Petihakis, G., Triantafyllou, G., Allen, I. J., Hoteit, I. and Dounas, C.: Modelling the spatial and temporal
1013 variability of the Cretan Sea ecosystem, *J. Mar. Syst.*, 36(3–4), 173–196, doi:10.1016/S0924-7963(02)00186-0, 2002.
- 1014 Petihakis, G., Triantafyllou, G., Korres, G., Tsiaras, K. and Theodorou, A.: Ecosystem modelling: Towards the
1015 development of a management tool for a marine coastal system part-II, ecosystem processes and biogeochemical
1016 fluxes, *J. Mar. Syst.*, 94(SUPPL.), 49–64, doi:10.1016/j.jmarsys.2011.11.006, 2012.



- 1017 Politikos, D. V., Tsiaras, K., Papatheodorou, G. and Anastasopoulou, A.: Modeling of floating marine litter
1018 originated from the Eastern Ionian Sea: Transport, residence time and connectivity, *Mar. Pollut. Bull.*, 150, 110727,
1019 doi:10.1016/j.marpolbul.2019.110727, 2020.
- 1020 Pouvreau, S., Bourles, Y., Lefebvre, S., Gangnery, A. and Alunno-Bruscia, M.: Application of a dynamic energy
1021 budget model to the Pacific oyster, *Crassostrea gigas*, reared under various environmental conditions, *J. Sea Res.*,
1022 56(2), 156–167, doi:10.1016/j.seares.2006.03.007, 2006.
- 1023 Prins, T. C., Smaal, A. C. and Pouwer, A. J.: Selective ingestion of phytoplankton by the bivalves *Mytilus edulis*
1024 L. and *Cerastoderma edule* (L.), *Hydrobiol. Bull.*, 25(1), 93–100, doi:10.1007/BF02259595, 1991.
- 1025 Qu, X., Su, L., Li, H., Liang, M. and Shi, H.: Assessing the relationship between the abundance and properties of
1026 microplastics in water and in mussels, *Sci. Total Environ.*, 621, 679–686, doi:10.1016/j.scitotenv.2017.11.284, 2018.
- 1027 Raitos, D. E., Korres, G., Triantafyllou, G., Petihakis, G., Pantazi, M., Tsiaras, K. and Pollani, A.: Assessing
1028 chlorophyll variability in relation to the environmental regime in Pagasitikos Gulf, Greece, *J. Mar. Syst.*, 94(SUPPL.),
1029 16–22, doi:10.1016/j.jmarsys.2011.11.003, 2012.
- 1030 Raitos, D. E., Lavender, S. J., Maravelias, C. D., Haralabous, J., Richardson, A. J. and Reid, P. C.: Identifying
1031 four phytoplankton functional types from space: An ecological approach, *Limnol. Oceanogr.*, 53(2), 605–613,
1032 doi:10.4319/lo.2008.53.2.0605, 2008.
- 1033 Raitos, D. E., Pradhan, Y., Lavender, S. J., Hoteit, I., Mcquatters-Gollop, A., Reid, P. C. and Richardson, A. J.:
1034 From silk to satellite: Half a century of ocean colour anomalies in the Northeast Atlantic, *Glob. Chang. Biol.*, 20(7),
1035 2117–2123, doi:10.1111/gcb.12457, 2014.
- 1036 Raitos, D. E., Reid, P. C., Lavender, S. J., Edwards, M. and Richardson, A. J.: Extending the SeaWiFS
1037 chlorophyll data set back 50 years in the northeast Atlantic, *Geophys. Res. Lett.*, 32(6), 1–4,
1038 doi:10.1029/2005GL022484, 2005.
- 1039 Ren, J. S.: Effect of food quality on energy uptake, *J. Sea Res.*, 62(2–3), 72–74,
1040 doi:10.1016/j.seares.2008.11.002, 2009.
- 1041 Riisgård, H. U., Egede, P. P. and Barreiro Saavedra, I.: Feeding Behaviour of the Mussel, *Mytilus edulis*: New
1042 Observations, with a Minireview of Current Knowledge, *J. Mar. Biol.*, 2011, 1–13, doi:10.1155/2011/312459, 2011.
- 1043 Riisgård, H. U., Kittner, C. and Seerup, D. F.: Regulation of opening state and filtration rate in filter-feeding
1044 bivalves (*Cardium edule*, *Mytilus edulis*, *Mya arenaria*) in response to low algal concentration, *J. Exp. Mar. Bio. Ecol.*,
1045 284(1–2), 105–127, doi:10.1016/S0022-0981(02)00496-3, 2003.
- 1046 Rios, L. M., Moore, C. and Jones, P. R.: Persistent organic pollutants carried by synthetic polymers in the ocean
1047 environment, *Mar. Pollut. Bull.*, 54(8), 1230–1237, doi:10.1016/j.marpolbul.2007.03.022, 2007.
- 1048 Rist, S., Steensgaard, I. M., Guven, O., Nielsen, T. G., Jensen, L. H., Møller, L. F. and Hartmann, N. B.: The fate
1049 of microplastics during uptake and depuration phases in a blue mussel exposure system, *Environ. Toxicol. Chem.*,
1050 38(1), 99–105, doi:10.1002/etc.4285, 2019.
- 1051 Romeo, T., Pietro, B., Pedà, C., Consoli, P., Andaloro, F. and Fossi, M. C.: First evidence of presence of plastic
1052 debris in stomach of large pelagic fish in the Mediterranean Sea, *Mar. Pollut. Bull.*, 95(1), 358–361,
1053 doi:10.1016/j.marpolbul.2015.04.048, 2015.
- 1054 Rosland, R., Strand, Alunno-Bruscia, M., Bacher, C. and Strohmeier, T.: Applying Dynamic Energy Budget
1055 (DEB) theory to simulate growth and bio-energetics of blue mussels under low seston conditions, *J. Sea Res.*, 62(2–3),
1056 49–61, doi:10.1016/j.seares.2009.02.007, 2009.
- 1057 Santana, M. F. M., Moreira, F. T., Pereira, C. D. S., Abessa, D. M. S. and Turra, A.: Continuous Exposure to
1058 Microplastics Does Not Cause Physiological Effects in the Cultivated Mussel *Perna perna*, *Arch. Environ. Contam.*
1059 *Toxicol.*, 74(4), 594–604, doi:10.1007/s00244-018-0504-3, 2018.
- 1060 Sarà, G., Kearney, M. and Helmuth, B.: Combining heat-transfer and energy budget models to predict thermal
1061 stress in Mediterranean intertidal mussels, *Chem. Ecol.*, 27(2), 135–145, doi:10.1080/02757540.2011.552227, 2011.
- 1062 Sarà, G., Milanese, M., Prusina, I., Sarà, A., Angel, D. L., Glamuzina, B., Nitzan, T., Freeman, S., Rinaldi, A.,
1063 Palmeri, V., Montalto, V., Lo Martire, M., Gianguzza, P., Arizza, V., Lo Brutto, S., De Pirro, M., Helmuth, B.,
1064 Murray, J., De Cantis, S. and Williams, G. A.: The impact of climate change on mediterranean intertidal communities:
1065 Losses in coastal ecosystem integrity and services, *Reg. Environ. Chang.*, 14(SUPPL.1), 5–17, doi:10.1007/s10113-
1066 012-0360-z, 2014.
- 1067 Sarà, G., Reid, G. K., Rinaldi, A., Palmeri, V., Troell, M. and Kooijman, S. A. L. M.: Growth and reproductive
1068 simulation of candidate shellfish species at fish cages in the Southern Mediterranean: Dynamic Energy Budget (DEB)
1069 modelling for integrated multi-trophic aquaculture, *Aquaculture*, 324–325, 259–266,
1070 doi:10.1016/j.aquaculture.2011.10.042, 2012.



- 1071 Saraiva, S., der Meer, J. van, Kooijman, S. A. L. M. and Sousa, T.: DEB parameters estimation for *Mytilus*
1072 *edulis*, *J. Sea Res.*, 66(4), 289–296, doi:10.1016/j.seares.2011.06.002, 2011b.
- 1073 Saraiva, S., van der Meer, J., Kooijman, S. A. L. M. and Sousa, T.: Modelling feeding processes in bivalves: A
1074 mechanistic approach, *Ecol. Modell.*, 222(3), 514–523, doi:10.1016/j.ecolmodel.2010.09.031, 2011a.
- 1075 Saraiva, S., Van Der Meer, J., Kooijman, S. A. L. M., Witbaard, R., Philippart, C. J. M., Hippler, D. and Parker,
1076 R.: Validation of a Dynamic Energy Budget (DEB) model for the blue mussel *Mytilus edulis*, *Mar. Ecol. Prog. Ser.*,
1077 463, 141–158, doi:10.3354/meps09801, 2012.
- 1078 Schwabl, P., Koppel, S., Königshofer, P., Bucsecs, T., Trauner, M., Reiberger, T. and Liebmann, B.: Detection of
1079 various microplastics in human stool: A prospective case series, *Ann. Intern. Med.*, 171(7), 453–457,
1080 doi:10.7326/M19-0618, 2019.
- 1081 Seuront, L., Nicastro, K. R., Zardi, G. I. and Goberville, E.: Decreased thermal tolerance under recurrent heat
1082 stress conditions explains summer mass mortality of the blue mussel *Mytilus edulis*, *Sci. Rep.*, 9(1),
1083 doi:10.1038/s41598-019-53580-w, 2019.
- 1084 Skoulikidis, N. T., Economou, A. N., Gritsalis, K. C. and Zogaris, S.: Rivers of the Balkans, *Rivers Eur.*, 421–
1085 466, doi:10.1016/B978-0-12-369449-2.00011-4, 2009.
- 1086 Smith, M., Love, D. C., Rochman, C. M. and Neff, R. A.: Microplastics in Seafood and the Implications for
1087 Human Health, *Curr. Environ. Heal. reports*, 5(3), 375–386, doi:10.1007/s40572-018-0206-z, 2018.
- 1088 Sprung, M.: Reproduction and fecundity of the mussel *mytilus edulis* at helgoland (North sea), *Helgoländer*
1089 *Meeresuntersuchungen*, 36(3), 243–255, doi:10.1007/BF01983629, 1983.
- 1090 Sukhotin, A. A. and Kulakowski, E. E.: Growth and population dynamics in mussels (*Mytilus edulis* L.) cultured
1091 in the White Sea, *Aquaculture*, 101(1–2), 59–73, doi:10.1016/0044-8486(92)90232-A, 1992.
- 1092 Sukhotin, A. A., Strelkov, P. P., Maximovich, N. V. and Hummel, H.: Growth and longevity of *Mytilus edulis*
1093 (L.) from northeast Europe, *Mar. Biol. Res.*, 3(3), 155–167, doi:10.1080/17451000701364869, 2007.
- 1094 Sussarellu, R., Suquet, M., Thomas, Y., Lambert, C., Fabioux, C., Pernet, M. E. J., Goic, N. Le, Quillien, V.,
1095 Mingant, C., Epelboin, Y., Corporeau, C., Guyomarch, J., Robbens, J., Paul-Pont, I., Soudant, P. and Huvet, A.: Oyster
1096 reproduction is affected by exposure to polystyrene microplastics, *Proc. Natl. Acad. Sci. U. S. A.*, 113(9), 2430–2435,
1097 doi:10.1073/pnas.1519019113, 2016.
- 1098 Tagliarolo, M. and McQuaid, C. D.: Sub-lethal and sub-specific temperature effects are better predictors of
1099 mussel distribution than thermal tolerance, *Mar. Ecol. Prog. Ser.*, 535, 145–159, doi:10.3354/meps11434, 2015.
- 1100 Teuten, E. L., Rowland, S. J., Galloway, T. S. and Thompson, R. C.: Potential for plastics to transport
1101 hydrophobic contaminants, *Environ. Sci. Technol.*, 41(22), 7759–7764, doi:10.1021/es071737s, 2007.
- 1102 Teuten, E. L., Saquing, J. M., Knappe, D. R. U., Barlaz, M. A., Jonsson, S., Björn, A., Rowland, S. J.,
1103 Thompson, R. C., Galloway, T. S., Yamashita, R., Ochi, D., Watanuki, Y., Moore, C., Viet, P. H., Tana, T. S.,
1104 Prudente, M., Boonyatumanond, R., Zakaria, M. P., Akkavong, K., Ogata, Y., Hirai, H., Iwasa, S., Mizukawa, K.,
1105 Hagino, Y., Imamura, A., Saha, M. and Takada, H.: Transport and release of chemicals from plastics to the
1106 environment and to wildlife, *Philos. Trans. R. Soc. B Biol. Sci.*, 364(1526), 2027–2045, doi:10.1098/rstb.2008.0284,
1107 2009.
- 1108 Theodorou, J. A., Viaene, J., Sorgeloos, P. and Tzovenis, I.: Production and Marketing Trends of the Cultured
1109 Mediterranean Mussel *Mytilus galloprovincialis* Lamarck 1819, in Greece , *J. Shellfish Res.*, 30(3), 859–874,
1110 doi:10.2983/035.030.0327, 2011.
- 1111 Thomas, Y., Mazurié, J., Alunno-Bruscia, M., Bacher, C., Bouget, J. F., Gohin, F., Pouvreau, S. and Struski, C.:
1112 Modelling spatio-temporal variability of *Mytilus edulis* (L.) growth by forcing a dynamic energy budget model with
1113 satellite-derived environmental data, *J. Sea Res.*, 66(4), 308–317, doi:10.1016/j.seares.2011.04.015, 2011.
- 1114 Thompson, R. C., Olson, Y., Mitchell, R. P., Davis, A., Rowland, S. J., John, A. W. G., McGonigle, D. and
1115 Russell, A. E.: Lost at Sea: Where Is All the Plastic?, *Science* (80-.), 304(5672), 838, doi:10.1126/science.1094559,
1116 2004.
- 1117 Triantafyllou, G., Petihakis, G. and Allen, I. J.: Assessing the performance of the Cretan Sea ecosystem model
1118 with the use of high frequency M3A buoy data set, *Ann. Geophys.*, 21(1), 365–375, doi:10.5194/angeo-21-365-2003,
1119 2003.
- 1120 Troost, T. A., Desclaux, T., Leslie, H. A., van Der Meulen, M. D. and Vethaak, A. D.: Do microplastics affect
1121 marine ecosystem productivity?, *Mar. Pollut. Bull.*, 135, 17–29, doi:10.1016/j.marpolbul.2018.05.067, 2018.
- 1122 Troost, T. A., Wijsman, J. W. M., Saraiva, S. and Freitas, V.: Modelling shellfish growth with dynamic energy
1123 budget models: An application for cockles and mussels in the Oosterschelde (southwest Netherlands), *Philos. Trans. R.*
1124 *Soc. B Biol. Sci.*, 365(1557), 3567–3577, doi:10.1098/rstb.2010.0074, 2010.



- 1125 Tsiaras, K. P., Petihakis, G., Kourafalou, V. H. and Triantafyllou, G.: Impact of the river nutrient load variability
1126 on the North Aegean ecosystem functioning over the last decades, *J. Sea Res.*, 86, 97–109,
1127 doi:10.1016/j.seares.2013.11.007, 2014.
- 1128 Vahl, O.: Efficiency of particle retention in *Mytilus edulis* L., *Ophelia*, 10(1), 17–25,
1129 doi:10.1080/00785326.1972.10430098, 1972.
- 1130 van Beusekom, J. E. E., Loebl, M. and Martens, P.: Distant riverine nutrient supply and local temperature drive
1131 the long-term phytoplankton development in a temperate coastal basin, *J. Sea Res.*, 61(1–2), 26–33,
1132 doi:10.1016/j.seares.2008.06.005, 2009.
- 1133 Van Cauwenberghe, L. and Janssen, C. R.: Microplastics in bivalves cultured for human consumption, *Environ.*
1134 *Pollut.*, 193, 65–70, doi:10.1016/j.envpol.2014.06.010, 2014.
- 1135 Van Cauwenberghe, L., Claessens, M., Vandegehuchte, M. B. and Janssen, C. R.: Microplastics are taken up by
1136 mussels (*Mytilus edulis*) and lugworms (*Arenicola marina*) living in natural habitats, *Environ. Pollut.*, 199, 10–17,
1137 doi:10.1016/j.envpol.2015.01.008, 2015.
- 1138 van der Veer, H. W., Cardoso, J. F. M. F. and van der Meer, J.: The estimation of DEB parameters for various
1139 Northeast Atlantic bivalve species, *J. Sea Res.*, 56(2), 107–124, doi:10.1016/j.seares.2006.03.005, 2006.
- 1140 van Haren, R. J. F., Schepers, H. E. and Kooijman, S. A. L. M.: Dynamic energy budgets affect kinetics of
1141 xenobiotics in the marine mussel *Mytilus edulis*, *Chemosphere*, 29(2), 163–189, doi:10.1016/0045-6535(94)90099-X,
1142 1994.
- 1143 Van Sebille, E., Wilcox, C., Lebreton, L., Maximenko, N., Hardesty, B. D., Van Franeker, J. A., Eriksen, M.,
1144 Siegel, D., Galgani, F. and Law, K. L.: A global inventory of small floating plastic debris, *Environ. Res. Lett.*, 10(12),
1145 124006, doi:10.1088/1748-9326/10/12/124006, 2015.
- 1146 Vandermeersch, G., Lourenço, H. M., Alvarez-Muñoz, D., Cunha, S., Diogène, J., Cano-Sancho, G., Sloth, J. J.,
1147 Kwadijk, C., Barcelo, D., Allegaert, W., Bekaert, K., Fernandes, J. O., Marques, A. and Robbens, J.: Environmental
1148 contaminants of emerging concern in seafood - European database on contaminant levels, *Environ. Res.*, 143, 29–45,
1149 doi:10.1016/j.envres.2015.06.011, 2015.
- 1150 Vlachogianni, T., Anastasopoulou, A., Fortibuoni, T., Ronchi, F. and Zeri, C.: Marine Litter Assessment in the
1151 Adriatic & Ionian Seas. IPA-Adriatic DeFishGear Project, MIO-ECSDE, HCMR and ISPRA. pp. 168 (ISBN: 978-
1152 960-6793-25-7), 2017.
- 1153 Von Moos, N., Burkhardt-Holm, P. and Köhler, A.: Uptake and effects of microplastics on cells and tissue of the
1154 blue mussel *Mytilus edulis* L. after an experimental exposure, *Environ. Sci. Technol.*, 46(20), 11327–11335,
1155 doi:10.1021/es302332w, 2012.
- 1156 Ward, J. E. and Kach, D. J.: Marine aggregates facilitate ingestion of nanoparticles by suspension-feeding
1157 bivalves, *Mar. Environ. Res.*, 68(3), 137–142, doi:10.1016/j.marenvres.2009.05.002, 2009.
- 1158 Ward, J. E. and Shumway, S. E.: Separating the grain from the chaff: Particle selection in suspension- and
1159 deposit-feeding bivalves, *J. Exp. Mar. Bio. Ecol.*, 300(1–2), 83–130, doi:10.1016/j.jembe.2004.03.002, 2004.
- 1160 Ward, J. E., Zhao, S., Holohan, B. A., Mladinich, K. M., Griffin, T. W., Wozniak, J. and Shumway, S. E.:
1161 Selective Ingestion and Egestion of Plastic Particles by the Blue Mussel (*Mytilus edulis*) and Eastern Oyster
1162 (*Crassostrea virginica*): Implications for Using Bivalves as Bioindicators of Microplastic Pollution, *Environ. Sci.*
1163 *Technol.*, 53(15), 8776–8784, doi:10.1021/acs.est.9b02073, 2019.
- 1164 Wegner, A., Besseling, E., Foekema, E. M., Kamermans, P. and Koelmans, A. A.: Effects of nanoplastyrene on
1165 the feeding behavior of the blue mussel (*Mytilus edulis* L.), *Environ. Toxicol. Chem.*, 31(11), 2490–2497,
1166 doi:10.1002/etc.1984, 2012.
- 1167 Widdows, J., Fieth, P. and Worrall, C. M.: Relationships between seston, available food and feeding activity in
1168 the common mussel *Mytilus edulis*, *Mar. Biol.*, 50(3), 195–207, doi:10.1007/BF00394201, 1979.
- 1169 Wieczorek, A. M., Morrison, L., Croot, P. L., Allcock, A. L., MacLoughlin, E., Savard, O., Brownlow, H. and
1170 Doyle, T. K.: Frequency of microplastics in mesopelagic fishes from the Northwest Atlantic, *Front. Mar. Sci.*, 5(FEB),
1171 doi:10.3389/fmars.2018.00039, 2018.
- 1172 Woods, M. N., Stack, M. E., Fields, D. M., Shaw, S. D. and Matrai, P. A.: Microplastic fiber uptake, ingestion,
1173 and egestion rates in the blue mussel (*Mytilus edulis*), *Mar. Pollut. Bull.*, 137, 638–645,
1174 doi:10.1016/j.marpolbul.2018.10.061, 2018.
- 1175 Zaldivar, J. M.: A general bioaccumulation DEB model for mussels. JRC Scientific and Technical Reports, EUR
1176 23626. Office for Official Publications of the European Communities: Luxembourg, ISBN 978-92-79-10943-0, ii, 31
1177 pp, 2008.



1178 Zeri, C., Adamopoulou, A., Bojanić Varezić, D., Fortibuoni, T., Kovač Viršek, M., Kržan, A., Mandić, M.,
1179 Mazziotti, C., Palatinus, A., Peterlin, M., Prvan, M., Ronchi, F., Siljic, J., Tutman, P. and Vlachogianni, T.: Floating
1180 plastics in Adriatic waters (Mediterranean Sea): From the macro- to the micro-scale, *Mar. Pollut. Bull.*, 136, 341–350,
1181 doi:10.1016/j.marpolbul.2018.09.016, 2018.

1182 Zhao, S., Ward, J. E., Danley, M. and Mincer, T. J.: Field-Based Evidence for Microplastic in Marine Aggregates
1183 and Mussels: Implications for Trophic Transfer, *Environ. Sci. Technol.*, 52(19), 11038–11048,
1184 doi:10.1021/acs.est.8b03467, 2018.

1185

1186

1187

1188

1189

1190

1191

1192

1193

1194

1195

1196

1197

1198

1199

1200

1201

1202

1203



1204 Tables & Figures

1205	$\frac{dE}{dt} = \dot{p}_a - \dot{p}_c$	(1)
1206	$\frac{dV}{dt} = \frac{k \cdot \dot{p}_c - [\dot{p}_M] \cdot V}{[E_g]}$	(2)
1207	$\frac{dR}{dt} = (1 - k) \cdot \dot{p}_c - \left[\frac{1-k}{k} \right] \cdot \min(V, V_p) \cdot [\dot{p}_M]$	(3)
1208	$\dot{p}_a = \{\dot{p}_{Am}\} \cdot f \cdot k(T) \cdot V^{\frac{2}{3}}$	(4)
1209	$f = \frac{X}{X + K_y}$, where $K_y = X_K \cdot \left(1 + \frac{Y}{Y_K}\right)$	(5)
1210	$\dot{p}_c = \frac{[E]}{[E_g] + k \cdot [E]} \cdot \left(\frac{[E_g] \cdot \{\dot{p}_{Am}\} \cdot k(T) \cdot V^{\frac{2}{3}}}{[E_m]} + [\dot{p}_M] \cdot V \right)$	(6)
1211	$[E] = \frac{E}{V}$	(7)
1212	$[\dot{p}_M] = k(T) \cdot [\dot{p}_M]_m$	(8)
1213	$k(T) = \frac{\exp\left(\frac{T_A - T_A}{T_I - T}\right)}{1 + \exp\left(\frac{T_{AL} - T_{AL}}{T_I - T}\right) + \exp\left(\frac{T_{AH} - T_{AH}}{T_H - T}\right)}$	(9)
1214	$L = \frac{1}{\delta_m V^{\frac{1}{3}}}$	(10)
1215	$W = d \cdot \left(V + \frac{E}{[E_g]} \right) + \frac{R}{\mu_E}$	(11)
1216	$\dot{C}_R = \frac{\{\dot{C}_{Rm}\}}{1 + \sum_i^n \frac{\rho_{Xi} \cdot \dot{p}_{XiF}}{\{\dot{p}_{XiFm}\}}} \cdot k(T) \cdot V^{\frac{2}{3}}$, $i = \begin{cases} 1 \text{ for CHL} \\ 2 \text{ for MPs} \end{cases}$ - a	(12) ^a
1217	$\dot{p}_{XiF} = \dot{C}_R \cdot X_i$	(13) ^a
1218	$\dot{p}_{XiU} = \frac{\rho_{Xi} \cdot \dot{p}_{XiF}}{1 + \sum_i^n \frac{\rho_{Xi} \cdot \dot{p}_{XiF}}{\{\dot{p}_{XiU}\}}}$	(14) ^a
1219	$\dot{J}_{pfi} = \dot{p}_{XiF} - \dot{p}_{XiU}$	(15) ^a
1220	$\dot{J}_f = \dot{p}_{X1U} - \dot{p}_A$	(16)
1221	$GSI = \frac{\frac{R}{\mu_E}}{d \cdot \left(V + \frac{E}{[E_g]} \right) + \frac{R}{\mu_E}}$	(17)

1222 Table 1. Dynamic energy budget model: equations. See Table 2 for model variables, Table 3 for parameters and Table
 1223 4 for initial values

1224 ^a notation refers to feeding equations handling each type of suspended matter separately ($i=1$ for algae and $i=2$ for
 1225 microplastics) where units transformation is applied when it is necessary (see Table 3).



1226

1227

1228	Variable	Description	Units
1229	V	Structural volume	cm^3
1230	E	Energy reserves	J
1231	R	Energy allocated to development	
1232		and reproduction	J
1233	C	Microplastics accumulation	particles individual ⁻¹
1234	\dot{p}_a	Assimilation energy rate	J d^{-1}
1235	\dot{p}_c	Utilization energy rate	J d^{-1}
1236	\dot{C}_R	Clearance rate	$\text{m}^3 \text{d}^{-1}$
1237	C_{env}	Microplastics concentration	particles L^{-1}
1238	\dot{p}_{XiF}	Filtration rate	J d^{-1} or g d^{-1}
1239	\dot{p}_{XiU}	Ingestion rate	J d^{-1} or g d^{-1}
1240	\dot{J}_{pfi}	Pseudofaeces production rate	J d^{-1} or g d^{-1}
1241	\dot{J}_f	Faeces production rate	J d^{-1}
1242	f	Functional response function	-
1243	X_i	Food or MPs density	mg chla m^{-3} or g m^{-3}
1244	$[\dot{p}_M]$	Maintenance costs	$\text{J cm}^{-3} \text{d}^{-1}$
1245	T	Temperature	K
1246	$k(T)$	Temperature dependence	-
1247	L	Shell length	cm
1248	W	Fresh tissue mass	g
1249	GSI	Gonado-somatic index	-

1250

Table 2. Dynamic energy budget model: variables

1251

1252

1253



1254	Parameter	Units	Description	Value	Reference
1255	$\{p_{Am}\}$	$\text{J cm}^{-2} \text{d}^{-1}$	Maximum surface area-specific assimilation rate	147.6	Van der Veer et al. (2006)
1256	$\{c_{Rm}\}$	$\text{m}^3 \text{cm}^{-2} \text{d}^{-1}$	Maximum surface area-specific clearance rate	0.096	Saraiva et al. (2011a)
1257	$\{p_{X_1Fm}\}$	$\text{mg chl a cm}^{-2} \text{d}^{-1}$	Algal maximum surface area-specific filtration rate* 0.1152		Rosland et al. (2009)
1258	$\{p_{X_2Fm}\}$	$\text{g cm}^{-2} \text{d}^{-1}$	Silt maximum surface area-specific filtration rate	3.5	Saraiva et al. (2011a)
1259	$\{p_{X_1Im}\}$	mg chl a d^{-1}	Algae maximum ingestion rate*	$3.12 \cdot 10^6$	Saraiva et al. (2011b)
1260	$\{p_{X_2Im}\}$	g d^{-1}	Silt maximum ingestion rate	0.11	Saraiva et al. (2011b)
1261	ρ_1	-	Algae binding probability	0.99	Saraiva et al. (2011a)
1262	ρ_2	-	Inorganic material binding probability	0.45	Saraiva et al. (2011a)
1263	X_K	mg chla m^{-3}	Half saturation coefficient	Calibrated	-
1264	T_A	K	Arrhenius temperature	5800	Van der Veer et al. (2006)
1265	T_I	K	Reference temperature	293	Van der Veer et al. (2006)
1266	T_L	K	Lower boundary of tolerance rate	275	Van der Veer et al. (2006)
1267	T_H	K	Upper boundary of tolerance rate	296	Van der Veer et al. (2006)
1268	T_{AL}	K	Rate of decrease of upper boundary	45430	Van der Veer et al. (2006)
1269	T_{AH}	K	Rate of decrease of lower boundary	31376	Van der Veer et al. (2006)
1270	$[p_M]_m$	$\text{J cm}^{-3} \text{d}^{-1}$	Volume specific maintenance costs	24	Van der Veer et al. (2006)
1271	$[E_G]$	J cm^{-3}	Volume specific growth costs	1900	Van der Veer et al. (2006)
1272	$[E_m]$	J cm^{-3}	Maximum energy density	2190	Van der Veer et al. (2006)
1273	k	-	Fraction of utilized energy spent on maintenance/growth	0.7	Van der Veer et al. (2006)
1274	V_p	cm^3	Volume at start of reproductive stage	0.06	Van der Veer et al. (2006)
1275	GSI_{th}	-	Gonado-somatic index triggering spawning	0.28	Van der Veer et al. (2006)
1276	δ_m	-	Shape coefficient	0.25	Casas & Bacher (2006)
1277	d	g cm^{-3}	Specific density	1.0	Kooijman (2000)
1278	μ_E	J g^{-1}	Energy content of reserves	6750	Casas & Bacher (2006)
1279	λ	J mg chl a^{-1}	Conversion factor	2387.73	Rosland et al. (2009)

1280 *Table 3. Dynamic energy budget model: parameters*

1281 *units mol C converted to mg CHL-a by multiplying with the factor $\frac{12 \cdot 10^3}{50}$ assuming Carbon:CHL-a ratio of 50
 1282 (Hatzonikolakis et al., 2017).



1283

1284

1285

Area	X_k value (mg m^{-3})	CHL-a range (mg m^{-3})	CHL-a mean (mg m^{-3})	Temperature range($^{\circ}\text{C}$)	Length after one year \pm SD (cm)	Reference
Maliakos Gulf	0.72	0.87-5.59	1.80	12.0-26.0	7.06 ± 0.46	Hatzonikolakis et al., 2017
Thermaikos Gulf	0.56	1.04-2.76	1.89	11.5-24.5	7.0 ± 0.47	Hatzonikolakis et al., 2017
Black Sea	Calibrated: 0.96	0.53-16.30	3.07	6.5-25.0	7.5 ± 0.1	Karayucel et al., 2010
Bizerte lagoon	3.829	4.00-7.70	5.20	12.0-28.0	7.26 ± 0.46	Béjaoui-Omri et al., 2014

1286

1287 *Table 4. Half saturation tuned values (X_k) and mussel growth data (Length) in different areas of the Mediterranean and*
 1288 *Black Seas.*

1289

1290

1291

1292

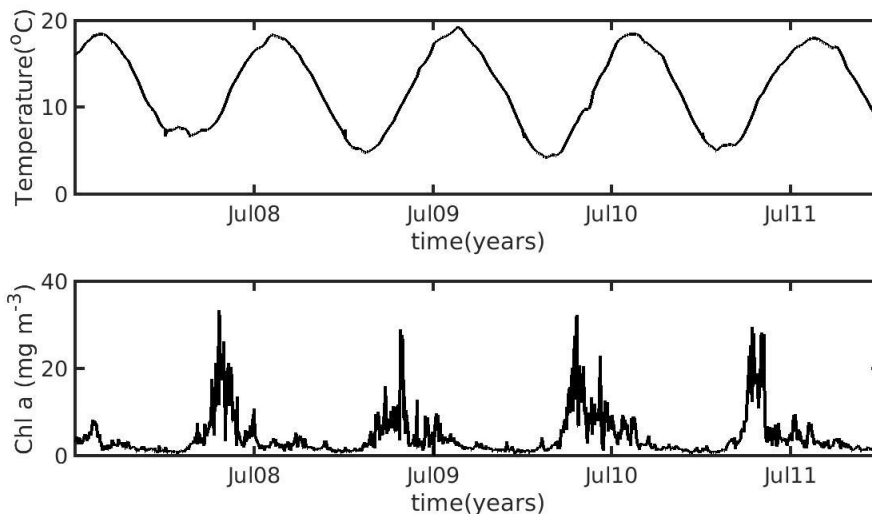
Northern Ionian Sea		North Sea	
Variable	Value	Variable	Value
Start date	20 Nov 2010	Start date	1 Jul 2014
L	0.85 cm	L	0.15 cm
W	0.1938 g	W	0.0055 g
V	0.0096 cm^3	V	$5.3 \cdot 10^{-5} \text{ cm}^3$
E	350 J	E	10 J
R	0 J	R	0 J
C	0 particles individual ⁻¹	C	0 particles individual ⁻¹

1302 *Table 5. Dynamic energy budget-accumulation model: initial values. L: shell length; W: fresh tissue mass; V: structural*
 1303 *volume; E: energy reserves; R: energy allocated to reproduction; C: Microplastics accumulation*

1304

1305

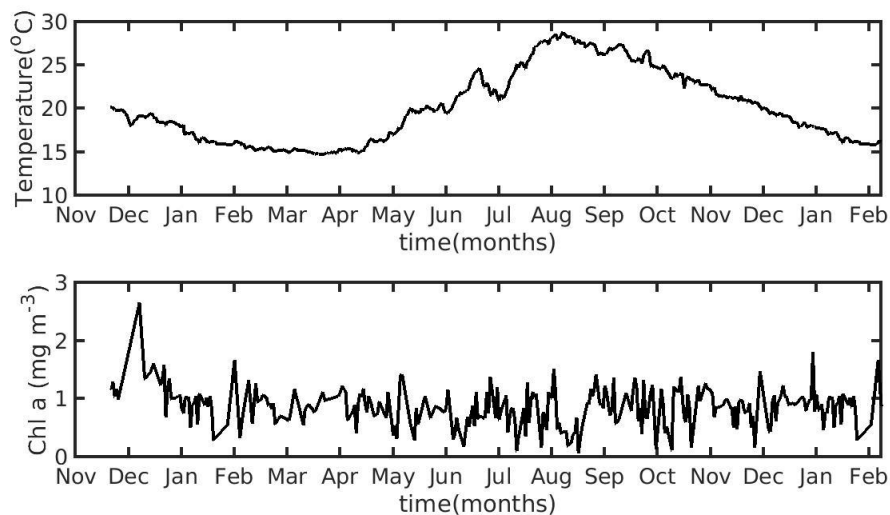
1306



1307

1308 *Fig. 1. Environmental data used for the forcing of the dynamic energy budget model in the North Sea simulation,*
1309 *showing temperature (top) and chlorophyll a concentration (bottom).*

1310



1311

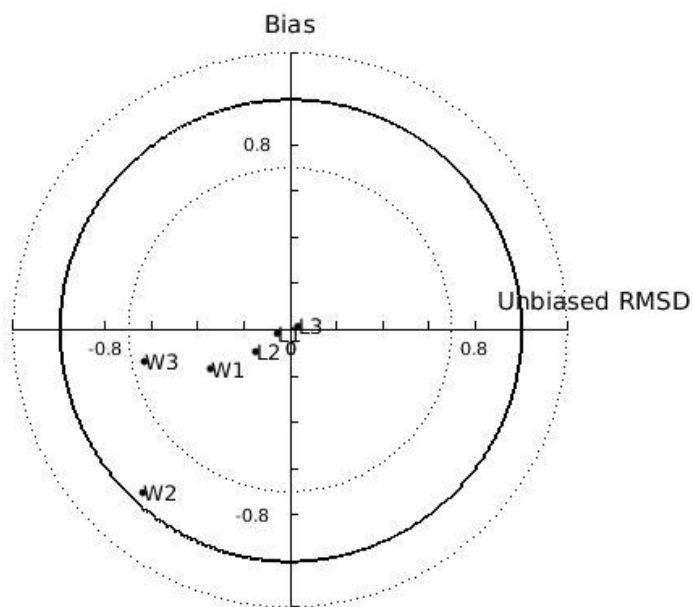
1312 *Fig. 2. Environmental data used for the forcing of the dynamic energy budget model in the Northern Ionian Sea*
1313 *simulation, showing temperature (top) and chlorophyll a concentration (bottom).*

1314

1315

1316

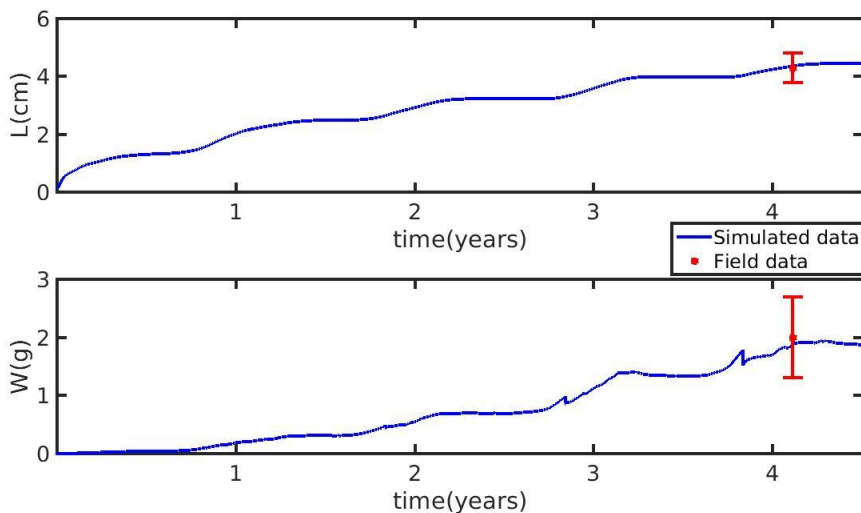
1317



1318

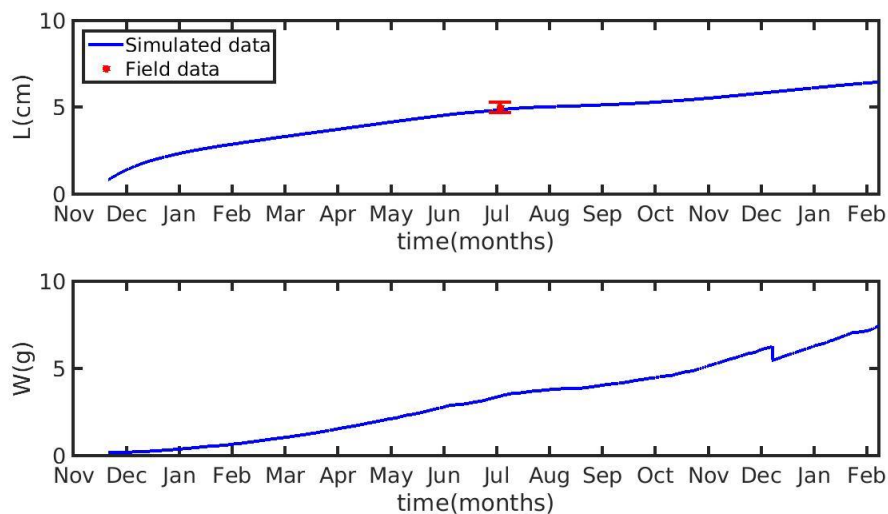
1319 *Fig. 3. Target diagram of simulated shell length (L) and fresh mass tissue weight (W) against field data from*
1320 *Thermaikos and Maliakos Gulf (eastern Mediterranean Sea), Black Sea and Bizerte Lagoon (southwestern*
1321 *Mediterranean Sea), using the power (L₁, W₁), exponential (L₂, W₂) and linear (L₃, W₃) function of the half saturation*
1322 *coefficient. The model bias is indicated on the y-axis while the unbiased root-mean-square-deviation (RMSD) is*
1323 *indicated on the x-axis.*

1324



1325

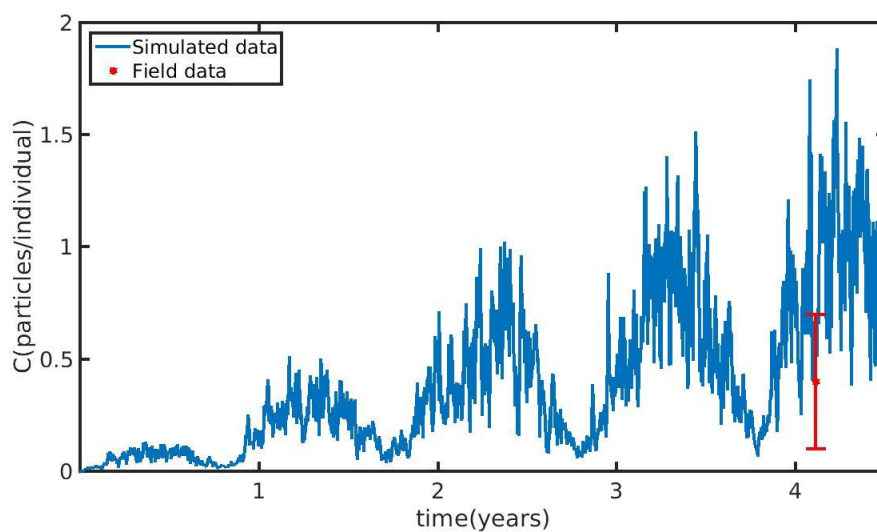
1326 *Fig. 4. Simulated mussel shell length (L) (top) and fresh tissue mass (W) (bottom) against North Sea data (red star:*
1327 *mean ± SD), using chlorophyll a (X = [CHL-a]) in the mussel diet.*



1328

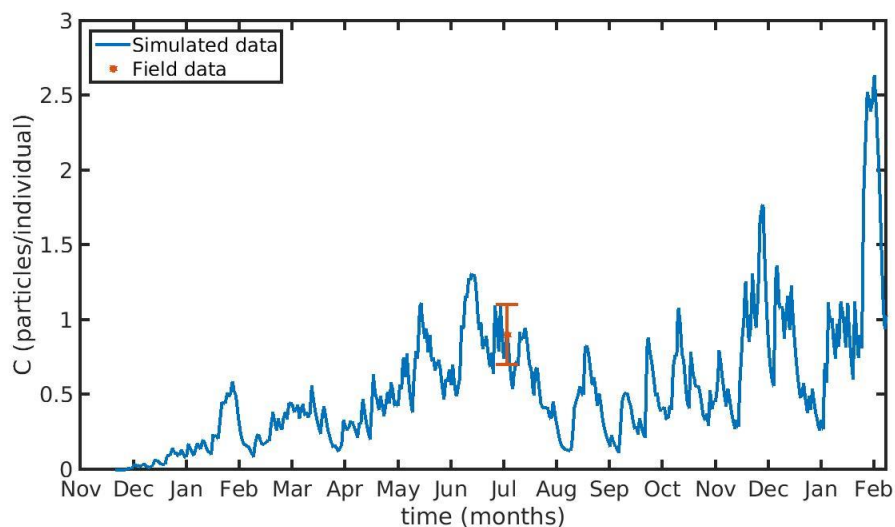
1329 *Fig. 5. Simulated mussel shell length (L) (top) and fresh tissue mass (W) (bottom) against Northern Ionian Sea data*
1330 *(red star: mean \pm SD), using chlorophyll a ($X = [CHL-a]$) in the mussel diet.*

1331



1332

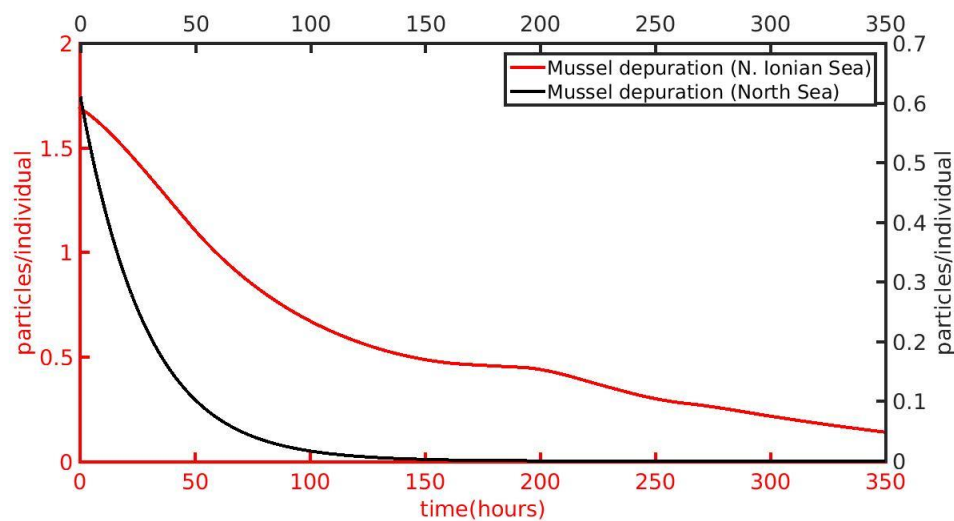
1333 *Fig. 6. Microplastics (MPs) accumulation by the mussel (blue line) against field data (red star: mean \pm SD), using daily*
1334 *environmental concentration of MPs (C_{env} mean value \pm SD: 0.4 ± 0.3 particles L^{-1}) in the North Sea.*



1335

1336 *Fig. 7. Microplastics (MPs) accumulation by the mussel (blue line) against field data (red star: mean value ± SD),*
1337 *using daily environmental concentration of MPs (C_{env} mean value ± SD: 0.0012 ± 0.024 particles L^{-1}) in the Northern*
1338 *Ionian Sea.*

1339



1340

1341 *Fig. 8. Depuration phase of the cultured *Mytilus galloprovincialis* (red line) and wild *Mytilus edulis* (black line) using*
1342 *zero environmental concentration of microplastics ($C_{env}=0$) after 1 year and 4 years of simulation time at the Northern*
1343 *Ionian Sea and North Sea respectively.*

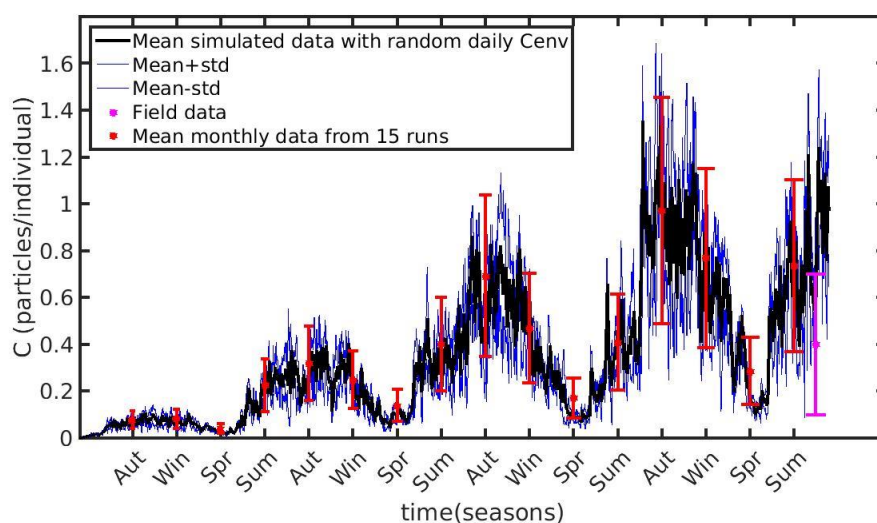
1344

1345

1346



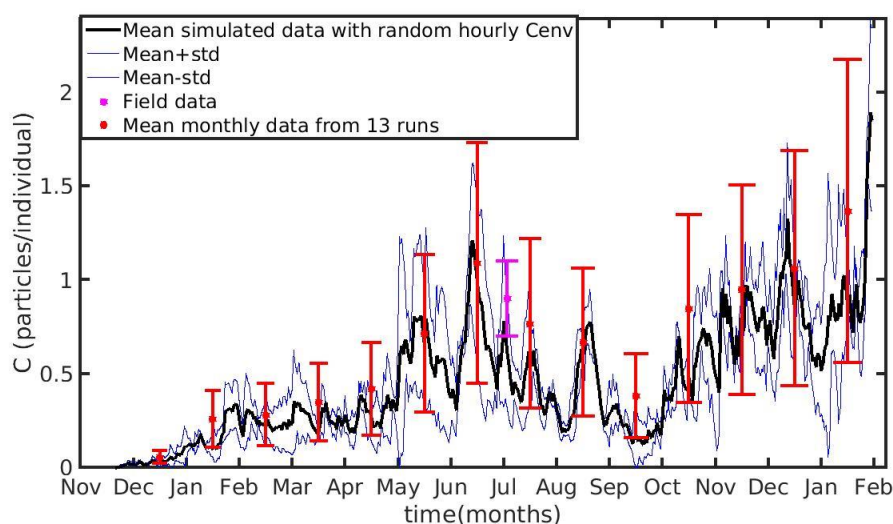
1347



1348

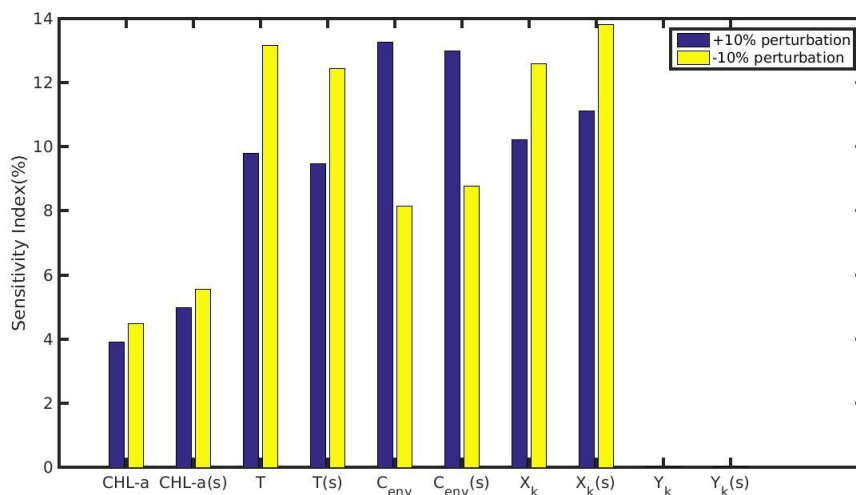
1349 *Fig.9. Mean seasonally values and standard deviation of microplastics (MPs) accumulation (red error bars: mean*
1350 *value ± SD) by the mussel in North Sea derived from 15 model runs with different constant values of environmental*
1351 *MPs concentration (C_{env} , range: 0.1-0.8 particles L^{-1}); Mean hourly simulated data (black line) and standard deviation*
1352 *(blue lines) of microplastics accumulation derived from 3 model runs with stochastic sequences of daily random C_{env}*
1353 *values.*

1354



1355

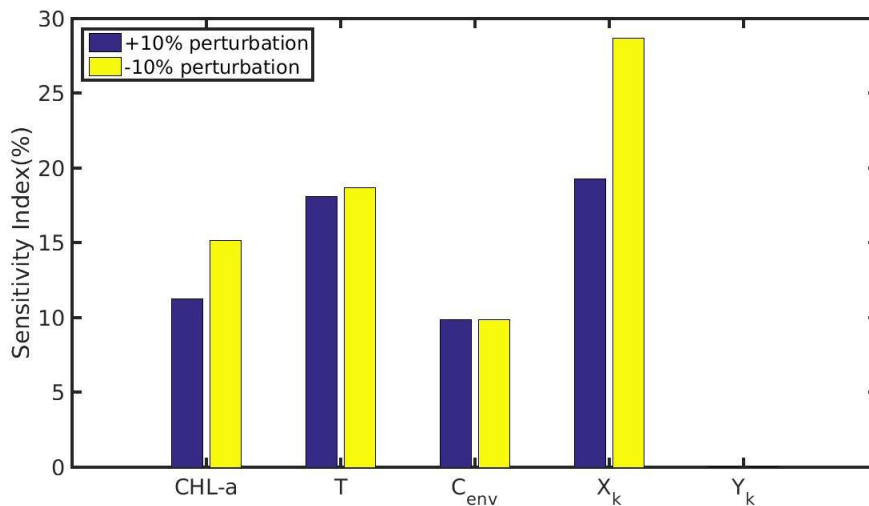
1356 *Fig. 10. Mean monthly values and standard deviation of microplastics accumulation (red error bars: mean value ± SD)*
1357 *by the mussel in Northern Ionian Sea derived from 13 model runs with different constant values of environmental*
1358 *MPs concentration (C_{env} , range: 0.0012-0.024 particles L^{-1}); Mean hourly simulated data (black line) and standard deviation*
1359 *(blue lines) of microplastics accumulation derived from 3 model runs with stochastic sequences of daily random C_{env}*
1360 *values.*



1361

1362 *Fig. 11. Sensitivity index of MPs accumulation on the wild mussel of the North Sea when variables (CHL-a,*
 1363 *temperature, C_{env}) and parameters (X_k, Y_k) are perturbed ± 10%. The notation (s) refers to the permanently submerged*
 1364 *mussel.*

1365



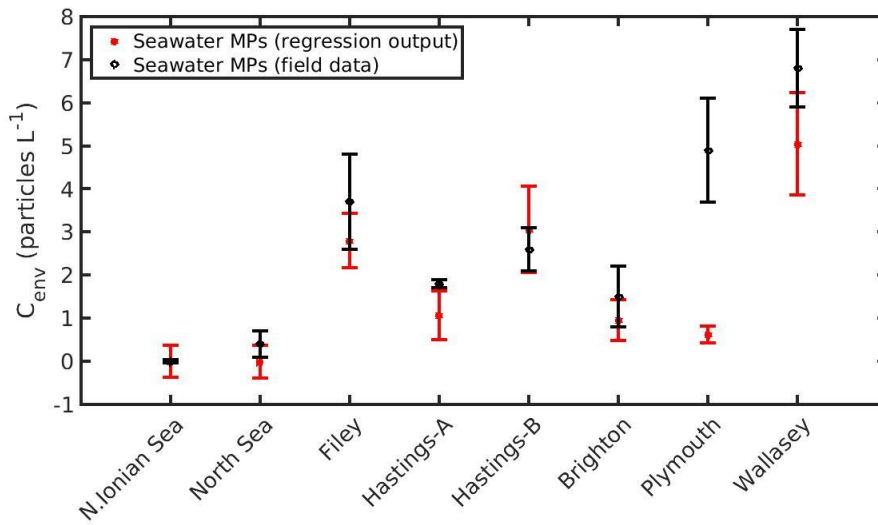
1366

1367 *Fig. 12. Sensitivity index of MPs accumulation on the cultured mussel of the Northern Ionian Sea when variables*
 1368 *(CHL-a, temperature, C_{env}) and parameters (X_k, Y_k) are perturbed ± 10%.*

1369

1370

1371



1372

1373 *Fig. 13. Prediction of seawater microplastics concentration by using Eq. 20 for the Northern Ionian Sea, North Sea*
1374 *(present study) and 6 areas around U.K. (Filey, Hastings-A&B, Brighton, Plymouth, Wallasey; Li et al. (2018)).*

1375